

# Compatible finite element methods for numerical weather prediction

Colin Cotter

Department of Mathematics  
Imperial College London

- Definition of 1D compatible finite element spaces.
- Absence of spurious pressure modes.
- Definition and examples of 2D compatible finite element spaces.
- Absence of spurious pressure modes, existence of steady geostrophic pressure modes.
- Energy-entropy conservation, PV conservation for nonlinear shallow-water equations.
- Some numerical tests.

# Why compatible finite elements?

## Compatible finite elements

Also known as:

- discrete differential forms (Bossavit, electromagnetism),
- Finite element exterior calculus (Arnold, elasticity).

Extends properties of C-grid but extra flexibility allows:

- 1 Higher-order consistency on arbitrary meshes,
- 2 Flexibility to alter DOF ratio between velocity and pressure,
- 3 No orthogonality constraint on meshes.

Discretise the 1D wave equation:

$$u_t + p_x = 0, \quad p_t + u_x = 0, \quad u(0) = u(1), \quad p(0) = p(1).$$

## The starting point

Represent  $u$  and  $p$  in some finite element space.

## How are different finite element spaces defined?

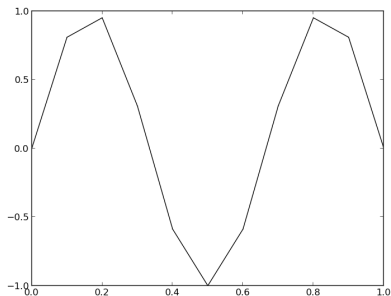
Finite element spaces are defined by:

- 1 The type of **polynomials** used in each element,
- 2 The degree of **continuity** across element boundaries.

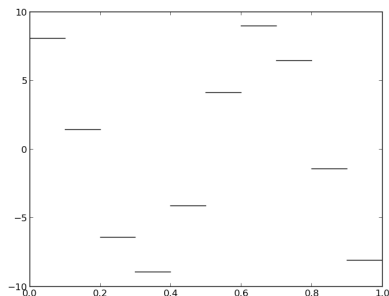
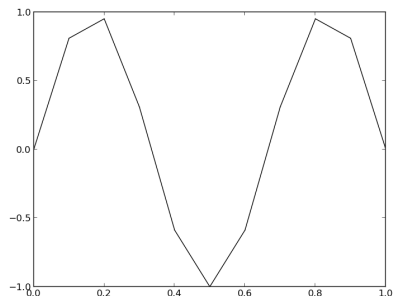


Example:

- 1  $p$  and  $u$  both **linear** functions in each element
- 2  $p$  and  $u$  both **continuous** across element boundaries



# Incompatibility



## Problem I: incompatibility

Writing  $u_t + p_x = 0$  doesn't work because:

- 1  $u$  is linear and continuous (P1).
- 2  $p_x$  is constant and discontinuous (P0).

## Approximation

Solution to **incompatibility** is to approximate  $p_x$  by the function  $v$  that is closest to  $p_x$  in  $P1$  (measured using  $L_2$  norm).

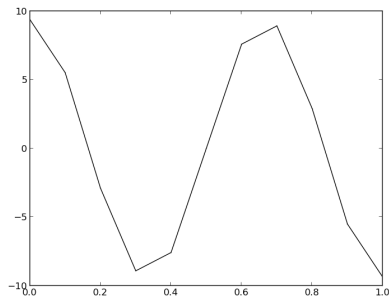
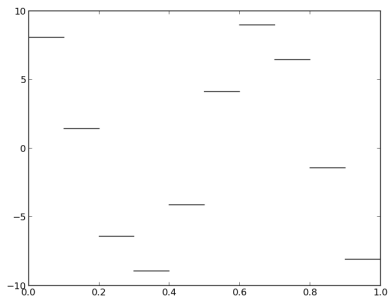
$$v = \operatorname{argmin}_{v \in P1} \|v - p_x\|_{L_2}^2 = \int_0^1 (v - p_x)^2 dx.$$

$$\text{Variational calculus} \implies \int_0^1 wv dx = \int_0^1 wp_x dx, \quad \forall w \in P1.$$

- 1 Expand  $w$  and  $v$  in a **basis** for  $P1$ .
- 2 Solve the resulting **sparse matrix system** for basis coefficients of  $v$ .

## Approximation

Solution to **incompatibility** is to approximate  $p_x$  by the function  $v$  that is closest to  $p_x$  in  $P_1$ .



# Building the equations

Unapproximated equations:

$$u_t + p_x = 0, \quad p_t + u_x = 0.$$

Minimisation:

$$u_t = \operatorname{argmin}_{u_t \in P1} \int_0^1 (u_t + p_x)^2 dx, \quad p_t = \operatorname{argmin}_{p_t \in P1} \int_0^1 (p_t + u_x)^2 dx.$$

Finite element discretisation:

$$\int_0^1 w u_t dx + \int_0^1 w p_x dx = 0, \quad \forall w \in P1,$$
$$\int_0^1 v p_t dx + \int_0^1 v u_x dx = 0, \quad \forall v \in P1.$$

## Spurious pressure modes

$p \in P1$  is a **spurious pressure mode** if:

- 1  $p \neq 0$ , and
- 2  $\int_0^1 w p_x dx \approx 0$ , for all  $w \in P1$ .

- If  $p \in P1$ , then  $p_x \in P_0$ .
- The **projection** of  $p_x$  into  $P_1$  **averages**  $p_x$  over two neighbouring elements.
- On a regular grid, a **zigzag pattern** in  $p$  has a vanishing discrete gradient.
- Identical to spurious pressure mode on **A-grid**.

# Smarter choice of finite element spaces

## Equal finite element spaces

The spurious pressure mode problem occurs whenever we use the **same finite element space** for  $u$  as  $p$ .

## Mixed finite element method

A **mixed finite element method** uses different finite element spaces for  $u$  and  $p$ .

- Already noticed that if  $u \in P1$ , then  $u_x \in P0$ .
- Choose  $u \in P1$ ,  $p \in P0$  to try to **avoid averaging**.
- We say that this choice of spaces is **compatible** with the derivative  $\partial/\partial x$ .

- Can now solve  $p_t + u_x = 0$  directly since  $p_t, u_x \in P0$ .
- Can't solve  $u_t + p_x = 0$  directly since  $P0$  functions are discontinuous.

## Solution

Integrate by parts in the integral form of the equations.

$$\int_0^1 w u_t dx + \int_0^1 w p_x dx = 0, \quad \forall w \in P1,$$

becomes

$$\int_0^1 w u_t dx - \int_0^1 w_x p dx + \underbrace{[wp]_0^1}_{=0} = 0, \quad \forall w \in P1.$$



# No spurious pressure modes

Proposition (Ladyzhenskaya/Babuška/Brezzi (LBB) condition for P1-P0)

*There exists a grid-independent constant  $C$  such that*

$$\max_{w \in P1} \frac{\left| \int_0^1 w_x p \, dx \right|}{\|w_x\|_{L_2}} \geq C \|p\|_{L_2}, \quad \forall p \in P0.$$

Proof.

Choose  $w$  with  $w_x = p$ , then

$$\max_{w \in P1} \frac{\left| \int_0^1 w_x p \, dx \right|}{\|w_x\|_{L_2}} \geq \frac{\int_0^1 p^2 \, dx}{\left( \int_0^1 p^2 \, dx \right)^{1/2}} = \left( \int_0^1 p^2 \, dx \right)^{1/2} = \|p\|_{L_2},$$

$\forall p \in P0$ . Hence  $C = 1$ . □

# No spurious pressure modes

Proposition (Ladyzhenskaya/Babuška/Brezzi (LBB) condition for P1-P0)

*There exists a grid-independent constant  $C$  such that*

$$\max_{w \in P1} \frac{\left| \int_0^1 w_x p \, dx \right|}{\|w_x\|_{L_2}} \geq C \|p\|_{L_2}, \quad \forall p \in P0.$$

Proof.

Choose  $w$  with  $w_x = p$ , then

$$\max_{w \in P1} \frac{\left| \int_0^1 w_x p \, dx \right|}{\|w_x\|_{L_2}} \geq \frac{\int_0^1 p^2 \, dx}{\left( \int_0^1 p^2 \, dx \right)^{1/2}} = \left( \int_0^1 p^2 \, dx \right)^{1/2} = \|p\|_{L_2},$$

$\forall p \in P0$ . Hence  $C = 1$ . □

# Building the equations II

Unapproximated equations:

$$u_t + p_x = 0, \quad p_t + u_x = 0.$$

Finite element discretisation:

$$\int_0^1 w u_t dx - \int_0^1 w_x p dx = 0, \quad \forall w \in P1,$$
$$\int_0^1 v p_t dx + \int_0^1 v u_x dx = 0, \quad \forall v \in P0,$$

or equivalently:

$$u_t + \tilde{\partial}_x p = 0, \quad p_t + u_x = 0.$$

## Proposition (Energy conservation)

The P1-P0 discretisation conserves the *energy*

$$E = \int_0^1 \frac{1}{2} u^2 + \frac{1}{2} p^2 dx.$$

Proof.

$$\begin{aligned} \dot{E} &= \int_0^1 uu_t dx + \int_0^1 pp_t dx, \\ &= \int_0^1 u_x p dx + \int_0^1 -pu_x dx = 0. \end{aligned}$$



## Proposition (Energy conservation)

The P1-P0 discretisation conserves the *energy*

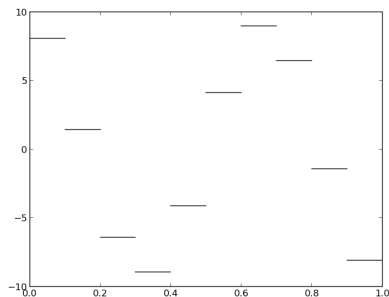
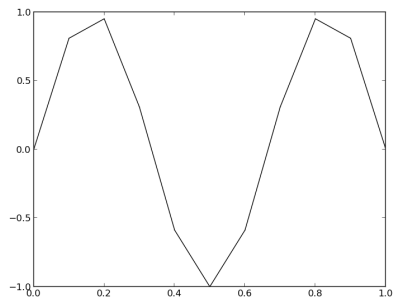
$$E = \int_0^1 \frac{1}{2} u^2 + \frac{1}{2} p^2 dx.$$

## Proof.

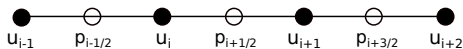
$$\begin{aligned} \dot{E} &= \int_0^1 uu_t dx + \int_0^1 pp_t dx, \\ &= \int_0^1 u_x p dx + \int_0^1 -pu_x dx = 0. \end{aligned}$$



# Connection to C-grid



Nodal basis for  $P1$  and  $P0$ :



# Equations for basis coefficients

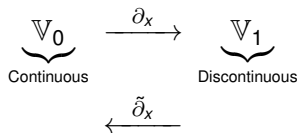
On **equispaced grid**:

$$\frac{1}{6} \left( \frac{\partial u_{i-1}}{\partial t} + 4 \frac{\partial u_i}{\partial t} + \frac{\partial u_{i+1}}{\partial t} \right) + \frac{p_{i+1/2} - p_{i-1/2}}{\Delta x} = 0,$$
$$\frac{\partial p_{i+1/2}}{\partial t} + \frac{u_{i+1} - u_i}{\Delta x} = 0.$$

- Slight alteration of **staggered finite difference method**.
- Need to **solve** system of equations to get  $\frac{\partial u_i}{\partial t}$ .
- This modification **maintains accuracy** on non-equispaced grids.

# General compatible finite elements in 1D

$$u \in \mathbb{V}_0, p \in \mathbb{V}_1.$$



General case:  $\mathbb{V}_0 = P_n$ ,  $\mathbb{V}_1 = P(n-1)_{DG}$ .



# Compatible finite element spaces in 2D

$$\underbrace{\mathbb{V}_0}_{\text{Continuous}} \xrightarrow{\nabla^\perp = (-\partial_y, \partial_x)} \underbrace{\mathbb{V}_1}_{\text{Continuous normals}} \xrightarrow{\nabla \cdot} \underbrace{\mathbb{V}_2}_{\text{Discontinuous}}$$

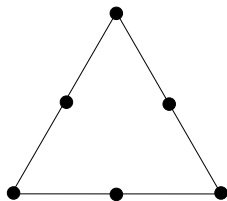
## Rules:

- 1  $\nabla \cdot$  maps from  $\mathbb{V}_1$  onto  $\mathbb{V}_2$ .
- 2  $\nabla^\perp$  maps from  $\mathbb{V}_0$  onto  $\ker(\nabla \cdot)$  in  $\mathbb{V}_1$ .

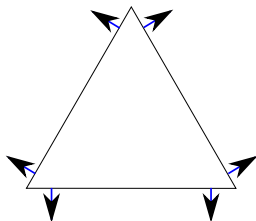
See: Arnold, Falk and Winther, Acta Numerica (2006) for history and general framework.

# Example FE spaces

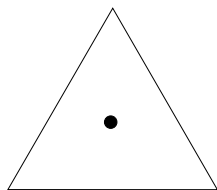
$$\underbrace{\mathbb{V}_0 = P_2}_{\text{Quadratic, Continuous}} \xrightarrow{\nabla^\perp} \underbrace{\mathbb{V}_1 = BDM1}_{\text{Linear, Continuous normals}} \xrightarrow{\nabla \cdot} \underbrace{\mathbb{V}_2 = P_0}_{\text{Constant, Discontinuous}}$$



Vorticity



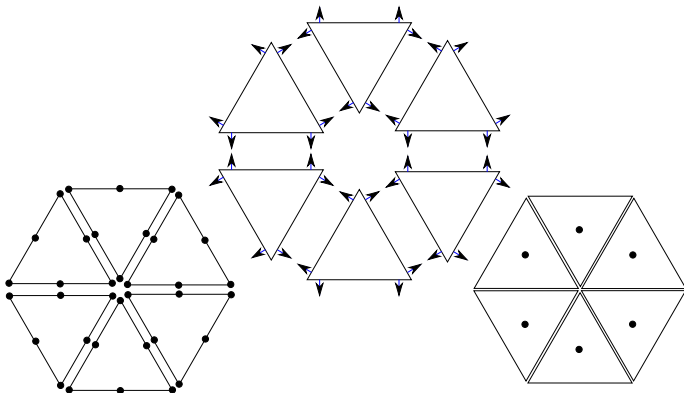
Velocity



Pressure

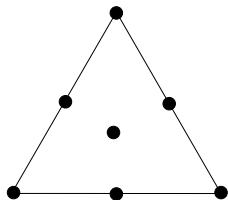
# Example FE spaces

$$\underbrace{\mathbb{V}_0 = P_2}_{\text{Quadratic, Continuous}} \xrightarrow{\nabla^\perp} \underbrace{\mathbb{V}_1 = BDM1}_{\text{Linear, Continuous normals}} \xrightarrow{\nabla \cdot} \underbrace{\mathbb{V}_2 = P_0}_{\text{Constant, Discontinuous}}$$

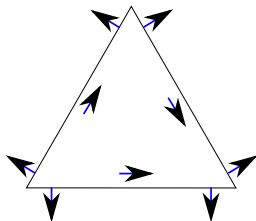


# Example FE spaces

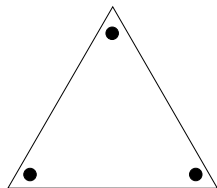
$$\underbrace{\mathbb{V}_0 = P2+}_{\text{Quadratic (+1 Cubic) Continuous}} \xrightarrow{\nabla^\perp} \underbrace{\mathbb{V}_1 = BDFM1}_{\text{Linear (+2 Quadratic) Cont. normals}} \xrightarrow{\nabla \cdot} \underbrace{\mathbb{V}_2 = P1_{DG}}_{\text{Linear Discontinuous}}$$



Vorticity



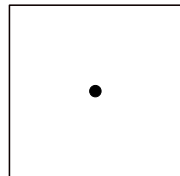
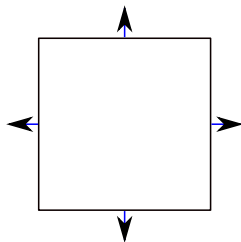
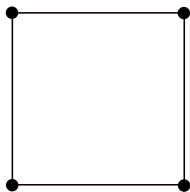
Velocity



Pressure

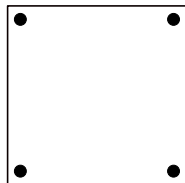
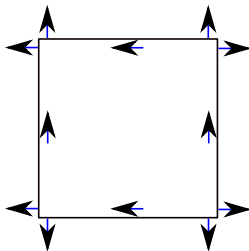
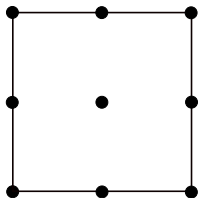
# Example FE spaces

$$\underbrace{\mathbb{V}_0 = Q1}_{\text{Bilinear Continuous}} \xrightarrow{\nabla^\perp} \underbrace{\mathbb{V}_1 = RT0}_{\text{Constant/Linear, Cont. normals}} \xrightarrow{\nabla \cdot} \underbrace{\mathbb{V}_2 = Q0_{DG}}_{\text{Constant, Discontinuous}}$$

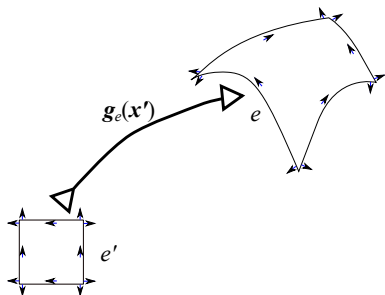


# Example FE spaces

$$\underbrace{\mathbb{V}_0 = Q_2}_{\text{Biquadratic Continuous}} \xrightarrow{\nabla^\perp} \underbrace{\mathbb{V}_1 = RT_1}_{\text{Bilinear/Biquadratic, Cont. normals}} \xrightarrow{\nabla \cdot} \underbrace{\mathbb{V}_2 = Q_1_{DG}}_{\text{Bilinear, Discontinuous}}$$



# Construction of $\mathbb{V}_1$



$$\mathbf{g}_e : e' \rightarrow e, \mathbf{x} = \mathbf{g}_e(\mathbf{x}').$$

## Definition (Piola transformation)

The Piola transformation  $\mathbf{u}' \mapsto \mathbf{u}$ :

$$\mathbf{u} \circ \mathbf{g}_e = \frac{1}{\det \frac{\partial \mathbf{g}_e}{\partial \mathbf{x}'}} \frac{\partial \mathbf{g}_e}{\partial \mathbf{x}'} \mathbf{u}'$$

$$\mathbf{u}' \cdot \mathbf{n}' dx' = \mathbf{g}_e^*(\mathbf{u} \cdot \mathbf{n} dx)$$

## Normal components

$$\int_f \mathbf{u}' \cdot \mathbf{n}' dx' = \int_{\mathbf{g}_e(f)} \mathbf{u} \cdot \mathbf{n} dx.$$

M. Rognes, CJC, D. Ham and A. McRae, *Automating the solution of PDEs on the sphere and other manifolds* (GMDD).

# Dual operators and projections

$$\mathbb{V}_0 \xrightarrow{\nabla^\perp = (-\partial_y, \partial_x)} \mathbb{V}_1 \xrightarrow{\nabla \cdot} \mathbb{V}_2$$
$$\xleftarrow{\tilde{\nabla}^\perp \cdot = (-\partial_y, \partial_x) \cdot} \quad \xleftarrow{\tilde{\nabla}}$$

where (assume no boundaries)

$$\int_{\Omega} \mathbf{w} \cdot \tilde{\nabla} h \, dx = - \int_{\Omega} \nabla \cdot \mathbf{w} h \, dx, \quad \forall \mathbf{w} \in \mathbb{V}_1$$
$$\int_{\Omega} \gamma \tilde{\nabla}^\perp \cdot \mathbf{u} \, dx = - \int_{\Omega} \nabla^\perp \gamma \cdot \mathbf{u} \, dx, \quad \forall \gamma \in \mathbb{V}_0.$$



# Dual operators and projections

$$\mathbb{V}_0 \xrightarrow{\nabla^\perp = (-\partial_y, \partial_x)} \mathbb{V}_1 \xrightarrow{\nabla \cdot} \mathbb{V}_2$$
$$\xleftarrow{\tilde{\nabla}^\perp \cdot = (-\partial_y, \partial_x) \cdot} \quad \xleftarrow{\tilde{\nabla}}$$

Also define projections  $\Pi_i$  into  $\mathbb{V}_i$ ,  $i = 0, 1, 2$  by:

$$\int_{\Omega} \gamma(\Pi_0 \alpha) \, dx = \int_{\Omega} \gamma \alpha \, dx, \quad \forall \gamma \in \mathbb{V}_0,$$
$$\int_{\Omega} \mathbf{w} \cdot (\Pi_1 \mathbf{F}) \, dx = \int_{\Omega} \mathbf{w} \cdot \mathbf{F} \, dx, \quad \forall \mathbf{w} \in \mathbb{V}_1,$$
$$\int_{\Omega} \phi(\Pi_2 \psi) \, dx = \int_{\Omega} \phi \psi \, dx, \quad \forall \phi \in \mathbb{V}_2.$$

# Dual operators and projections

$$\begin{array}{ccccc} \mathbb{V}_0 & \xrightarrow{\nabla^\perp} & \mathbb{V}_1 & \xrightarrow{\nabla \cdot} & \mathbb{V}_2 \\ & & \xleftarrow{\tilde{\nabla}^\perp} & & \xleftarrow{\tilde{\nabla}} \end{array}$$

## Properties

- 1  $\tilde{\nabla}^\perp \cdot \Pi_1 \mathbf{u}^\perp = \Pi_0 \nabla \cdot \mathbf{u}$  for  $\mathbf{u} \in \mathbb{V}_1$ ,
- 2  $\Pi_1 \nabla \psi = \tilde{\nabla} \Pi_2 \psi$  for  $\psi \in \mathbb{V}_0$ ,
- 3  $\tilde{\nabla}^\perp \cdot \tilde{\nabla} = 0$  (of course  $\nabla \cdot \nabla^\perp = 0$ ).

# Application to linearised RWSE

$$\mathbf{u}_t + f\Pi_1 \mathbf{u}^\perp + g\tilde{\nabla} h = 0, \quad h_t + H\nabla \cdot \mathbf{u} = 0, \quad \mathbf{u} \in \mathbb{V}_1, h \in \mathbb{V}_2.$$

Proposition (Ladyzhenskaya/Babuška/Brezzi (LBB) condition for 2D)

*There exists a grid-independent constant  $C$  such that*

$$\max_{\mathbf{w} \in \mathbb{V}_1} \frac{|\int_{\Omega} \nabla \cdot \mathbf{w} p \, dx|}{\|\nabla \cdot \mathbf{w}\|_{L_2}} \geq C \|p\|_{L_2}, \quad \forall p \in \mathbb{V}_2.$$

Proof.

Choose  $\mathbf{w}$  with  $\nabla \cdot \mathbf{w} = p$ , then

$$\max_{\mathbf{w} \in \mathbb{V}_1} \frac{|\int_{\Omega} \nabla \cdot \mathbf{w} p \, dx|}{\|\nabla \cdot \mathbf{w}\|_{L_2}} \geq \frac{\int_{\Omega} p^2 \, dx}{(\int_{\Omega} p^2 \, dx)^{1/2}} = (\int_{\Omega} p^2 \, dx)^{1/2} = \|p\|_{L_2},$$

$\forall p \in \mathbb{V}_2$ . Hence  $C = 1$ . □

# Application to linearised RWSE

$$\mathbf{u}_t + f\Pi_1 \mathbf{u}^\perp + g\tilde{\nabla} h = 0, \quad h_t + H\nabla \cdot \mathbf{u} = 0, \quad \mathbf{u} \in \mathbb{V}_1, h \in \mathbb{V}_2.$$

Proposition (Ladyzhenskaya/Babuška/Brezzi (LBB) condition for 2D)

*There exists a grid-independent constant  $C$  such that*

$$\max_{\mathbf{w} \in \mathbb{V}_1} \frac{|\int_{\Omega} \nabla \cdot \mathbf{w} p \, dx|}{\|\nabla \cdot \mathbf{w}\|_{L_2}} \geq C \|p\|_{L_2}, \quad \forall p \in \mathbb{V}_2.$$

Proof.

Choose  $\mathbf{w}$  with  $\nabla \cdot \mathbf{w} = p$ , then

$$\max_{\mathbf{w} \in \mathbb{V}_1} \frac{|\int_{\Omega} \nabla \cdot \mathbf{w} p \, dx|}{\|\nabla \cdot \mathbf{w}\|_{L_2}} \geq \frac{\int_{\Omega} p^2 \, dx}{(\int_{\Omega} p^2 \, dx)^{1/2}} = (\int_{\Omega} p^2 \, dx)^{1/2} = \|p\|_{L_2},$$

$\forall p \in \mathbb{V}_2$ . Hence  $C = 1$ . □

$$\mathbf{u}_t + f\Pi_1\mathbf{u}^\perp + g\tilde{\nabla}h = 0, \quad h_t + H\nabla \cdot \mathbf{u} = 0, \quad \mathbf{u} \in \mathbb{V}_1, h \in \mathbb{V}_2.$$

Geostrophic steady states:

- 1 If  $\nabla \cdot \mathbf{u} = 0$ , then  $\mathbf{u} = \nabla^\perp\psi$ ,  $\psi \in \mathbb{V}_0$ .
- 2 Choose  $h = f\Pi_2\psi/g$ , then
$$f\Pi_1(\mathbf{u}^\perp) = -f\Pi_1\nabla\psi = -f\tilde{\nabla}\Pi_2\psi = -g\tilde{\nabla}h.$$

# Application to nonlinear RSWE

$$\mathbf{u}_t + f \underbrace{(q\mathbf{u}h)}_{=\mathbf{Q}}^\perp + \nabla \left( gh + |\mathbf{u}|^2/2 \right) = 0, \quad h_t + \nabla \cdot \underbrace{(\mathbf{u}h)}_{=\mathbf{F}} = 0.$$

$$\mapsto \mathbf{u}_t + f\Pi_1 \mathbf{Q}^\perp + g\check{\nabla} \left( h + \Pi_2 |\mathbf{u}|^2/2 \right) = 0, \quad h_t + \nabla \cdot \mathbf{F} = 0,$$

for  $\mathbf{u}, \mathbf{F} \in \mathbb{V}_1$ ,  $h \in \mathbb{V}_2$  and some  $\mathbf{Q}$ .

## Strategy from Arakawa and Lamb, Sadourny

- 1 Apply natural curl to get vorticity equation.
- 2 Map  $h$  to vertices to evaluate PV.
- 3 Diagnose PV flux  $\mathbf{Q}$  via  $\mathbf{F}$  and insert into velocity equation.

# Implied PV equation

$$\mathbf{u}_t + f\Pi_1 \mathbf{Q}^\perp + \tilde{\nabla} \left( gh + \Pi_2 |\mathbf{u}|^2/2 \right) = 0,$$

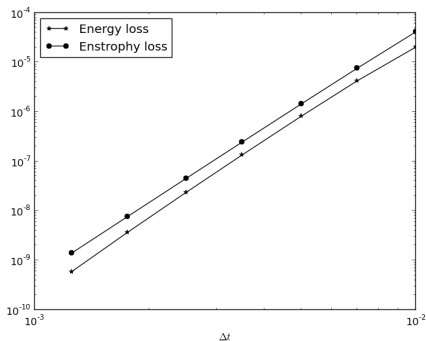
$$\text{Apply } \tilde{\nabla}^\perp \cdot : \quad \tilde{\nabla}^\perp \mathbf{u}_t + \tilde{\nabla}^\perp \cdot \mathbf{Q}^\perp + \underbrace{\tilde{\nabla}^\perp \cdot \tilde{\nabla}}_{=0} (gh + \Pi_2 |\mathbf{u}|^2/2) = 0.$$

PV  $q \in \mathbb{V}_0$  defined by  $\Pi_0(qh) = \tilde{\nabla}^\perp \cdot \mathbf{u} + \Pi_0(f)$ .

$$\text{Get } \frac{\partial}{\partial t} \Pi_0(qh) + \tilde{\nabla}^\perp \cdot \mathbf{Q}^\perp = 0.$$

Usual continuous finite element discretisation:

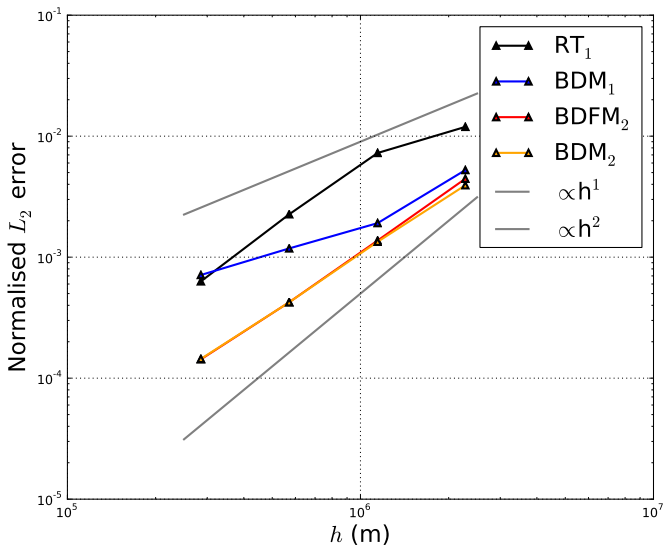
$$\int_{\Omega} \gamma(qh)_t \, dx - \int_{\Omega} \nabla \gamma \cdot \mathbf{Q} \, dx = 0.$$



## McRae and Cotter (submitted to QJRMS)

- 1 The choice  $\mathbf{F} = \Pi_1(h\mathbf{u})$  and  $\mathbf{Q} = \mathbf{F}q$  conserves energy and enstrophy.
- 2 The choice  $\mathbf{F} = \Pi_1(h\mathbf{u})$  and  $\mathbf{Q} = \mathbf{F}(q - (\tau/h)\mathbf{F} \cdot \nabla q)$  conserves energy and dissipates enstrophy (APVM).
- 3 Both choices preserve constant  $q$  field for any initial  $h$ .





From Andrew McRae, using energy conserving, enstrophy dissipating (APVM) formulation.

# Implicit timestepping setup

$$\mathbf{u}_t + \underbrace{(\mathbf{u}Dq)}_{\mathbf{Q}}^\perp + \nabla \left( gD + \frac{1}{2}|\mathbf{u}|^2 \right) = 0,$$
$$D_t + \nabla \cdot \underbrace{(\mathbf{u}D)}_{\mathbf{F}} = 0.$$

Crank-Nicholson:

$$\frac{\mathbf{u}^{n+1} - \mathbf{u}^n}{\Delta t} + \overline{\mathbf{Q}}^\perp + \nabla \left( g\overline{D} + \frac{1}{2}|\overline{\mathbf{u}}|^2 \right) = 0.$$

Solve  $D_t + \nabla \cdot (\overline{\mathbf{u}}D) = 0,$   
 $(qD)_t + \nabla \cdot (\overline{\mathbf{u}}Dq) = 0,$  from  $t^n$  until  $t^{n+1},$

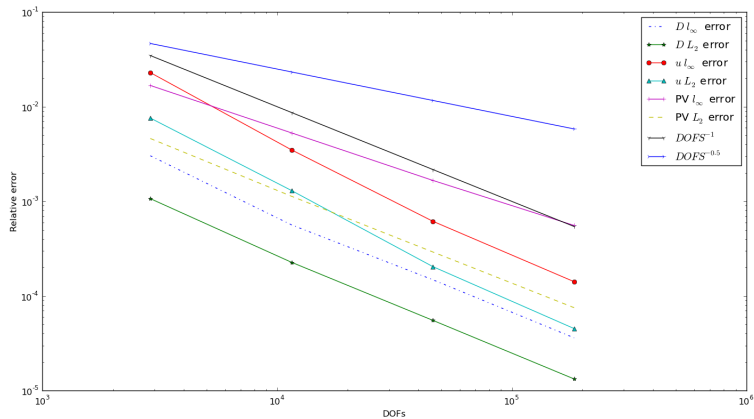
Then  $\overline{\mathbf{Q}} = \overline{\overline{\mathbf{u}}Dq}.$

Preserves constant  $q$  fields.

# Implementation details

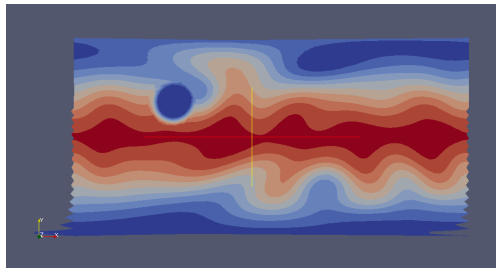
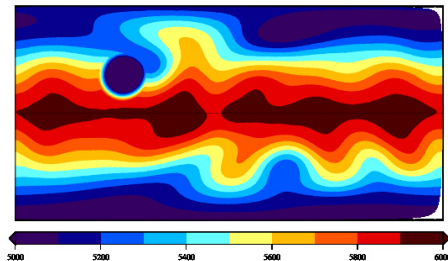
- Scheme implemented on cubic “bendy” elements, all terms except for mass matrices are topological only (local element matrices independent of coordinates).
- P2(bubble)-BDFM1-P1DG spaces used.
- 3rd order in time SSPRK-DG used for layer depth (can locally reconstruct  $\mathbf{F}$ ).
- 2 level, 3rd order in time  $\bar{T}(2, 3)$  Taylor-Galerkin scheme of Safjan and Oden (1995) used for PV (2 CG mass-matrix-like solves per timestep).
- 4 quasi-Newton iterations per timestep, and  $\theta = 1/2$ .
- Helmholtz equation formed by hybridisation.

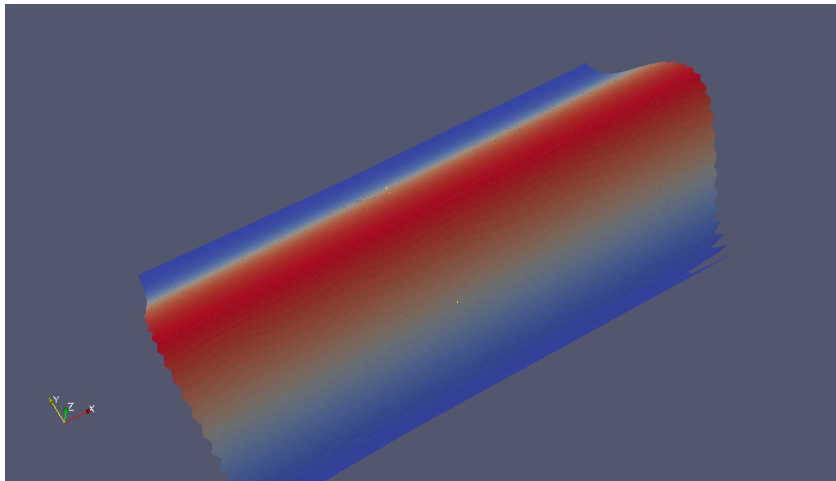
## Solid rotation testcase.



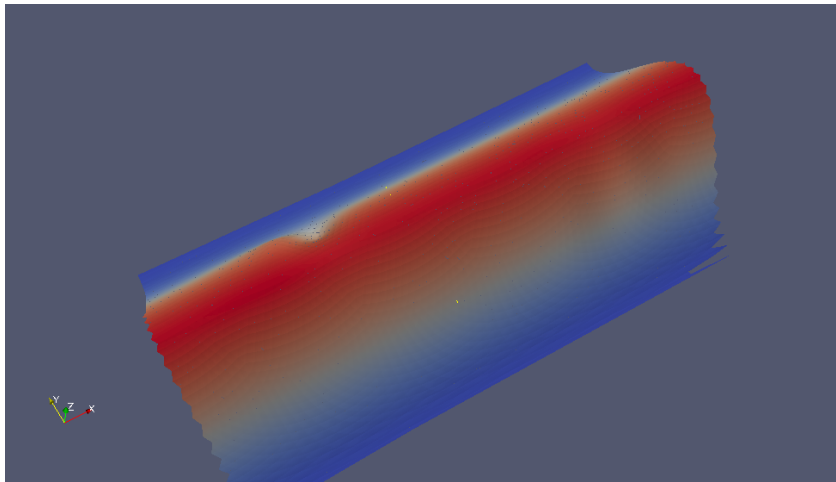
# Testcases

Mountain test case (Grid 5, 46080 DOFs).

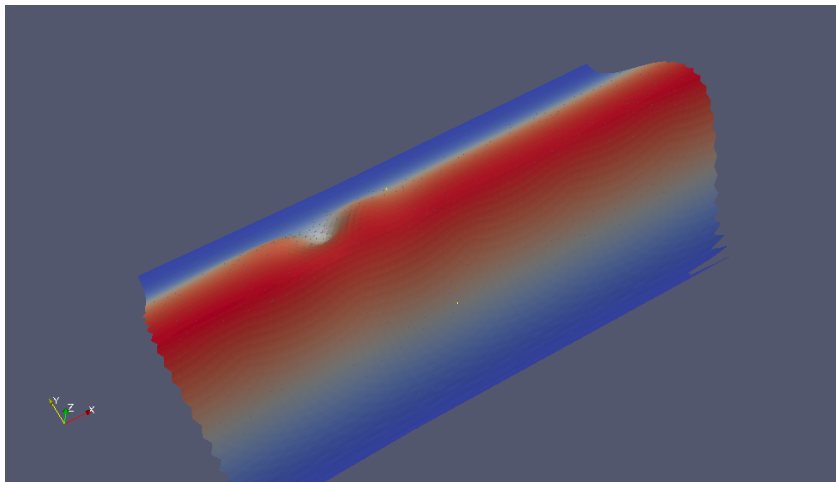




0

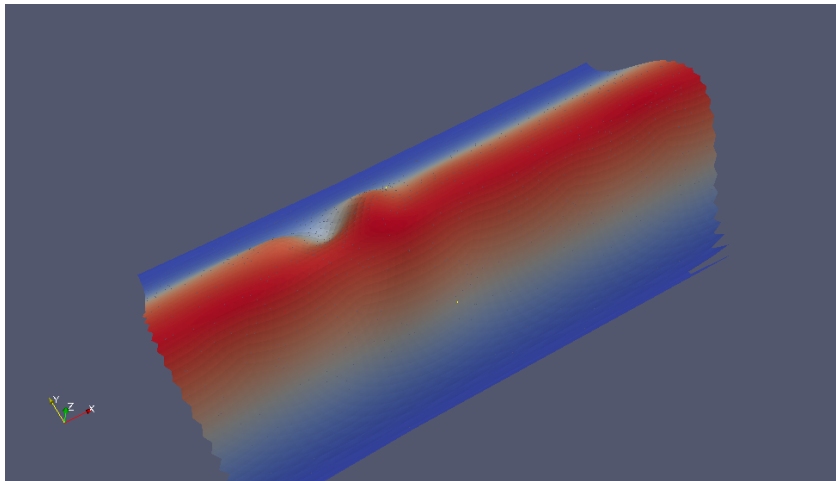


1

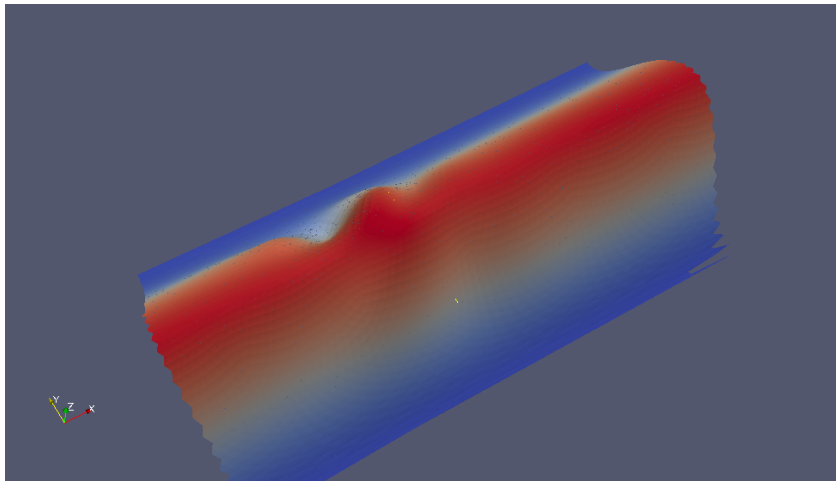


2

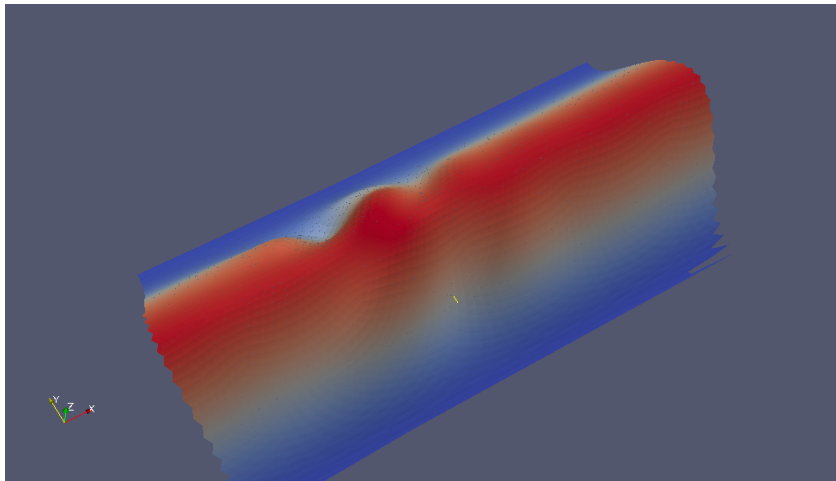




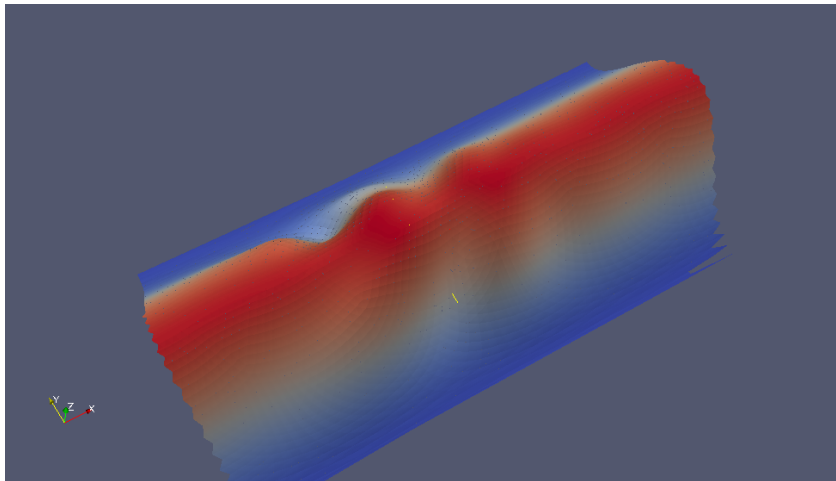
3



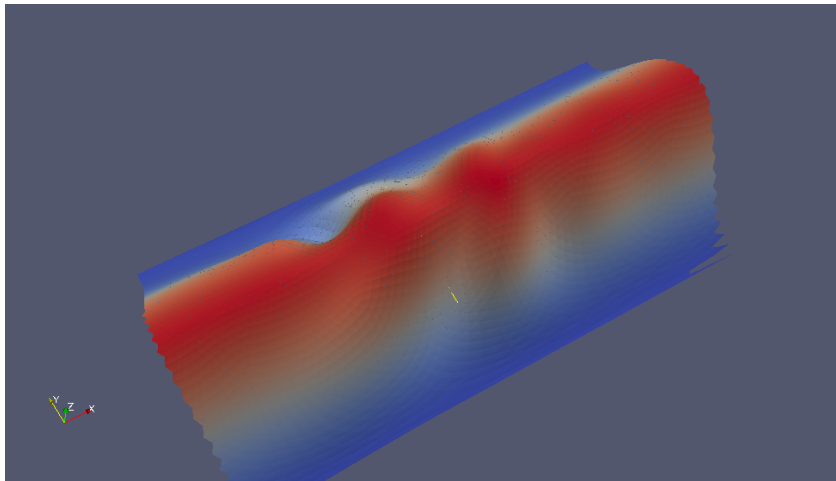
4



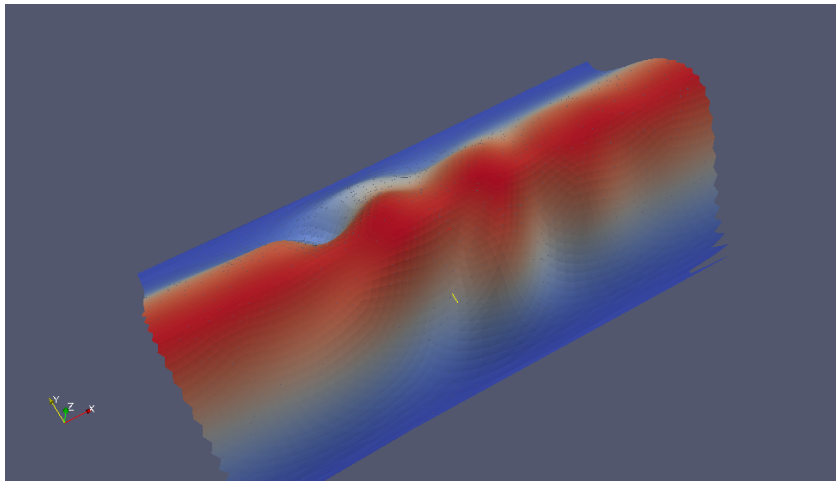
5



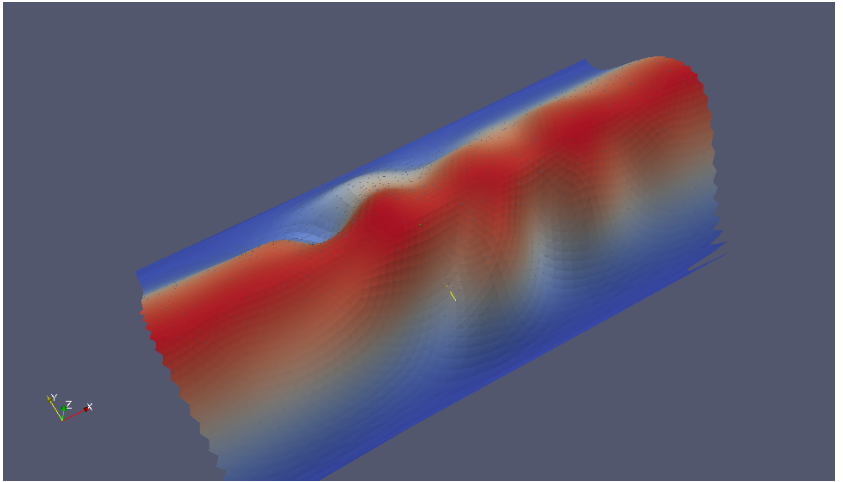
6



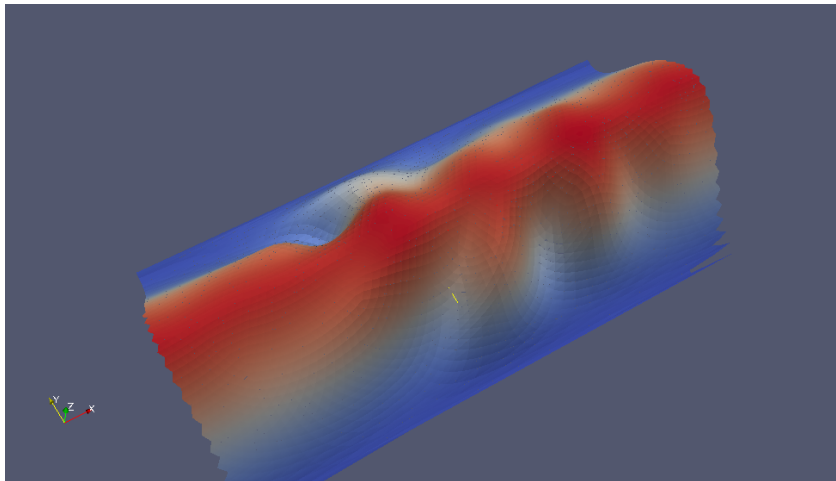
7



8

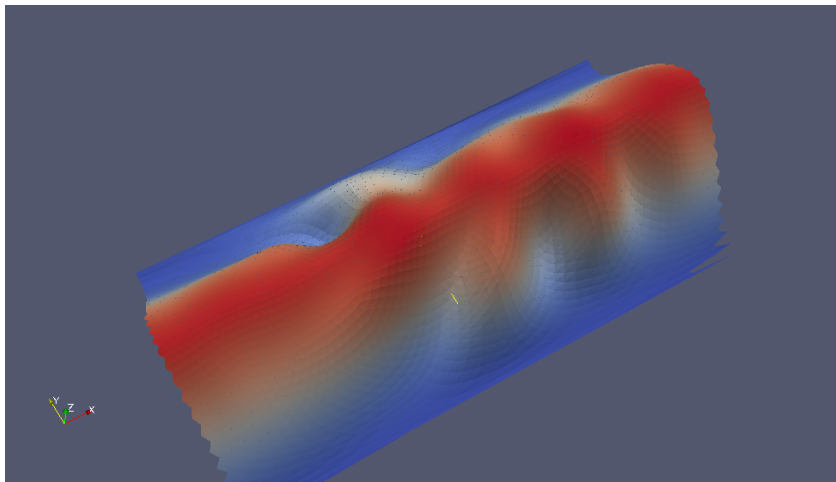


9

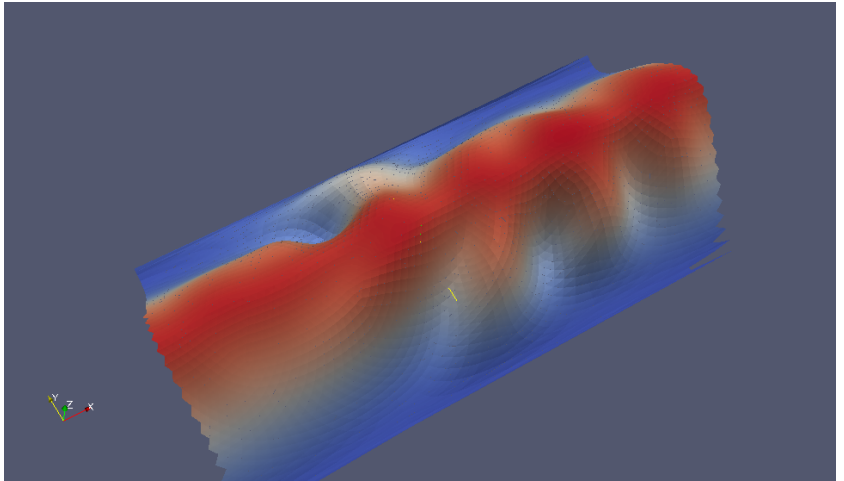


10

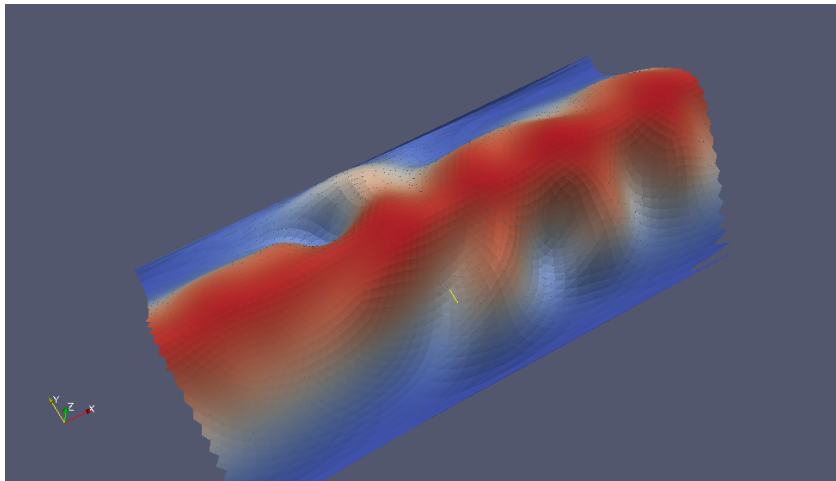




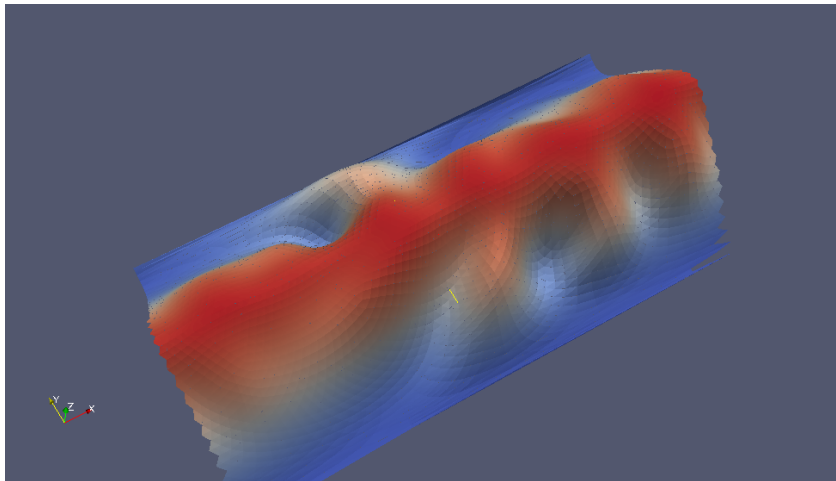
11



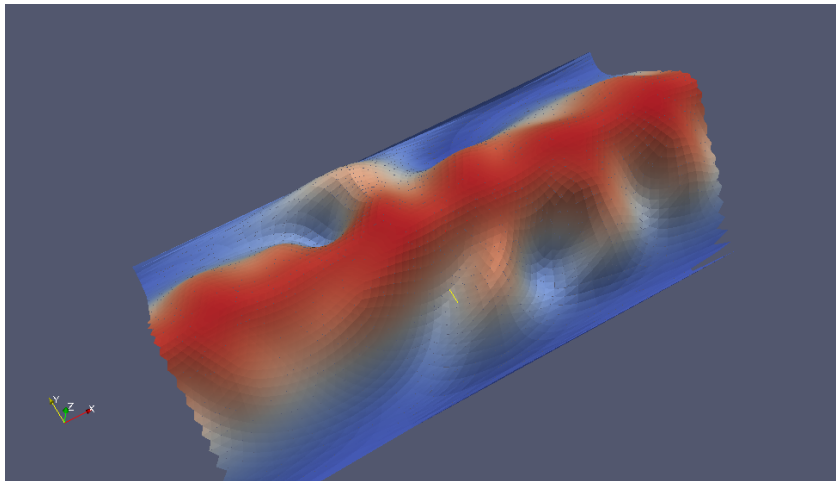
12



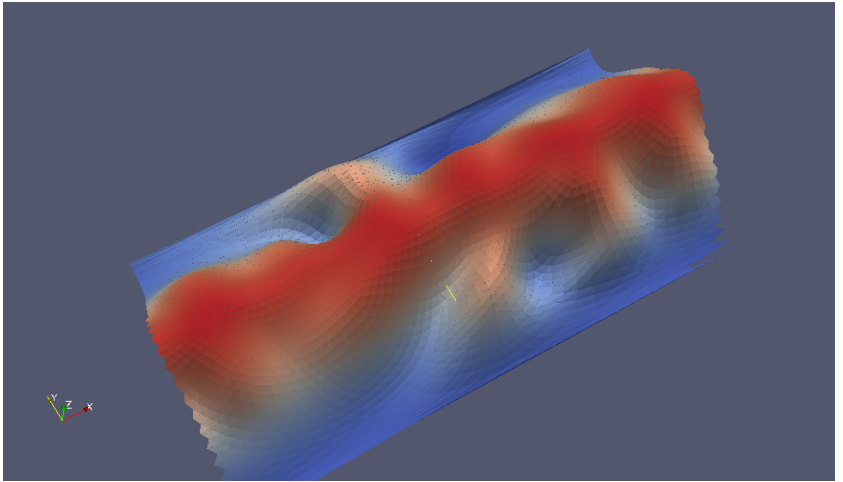
13



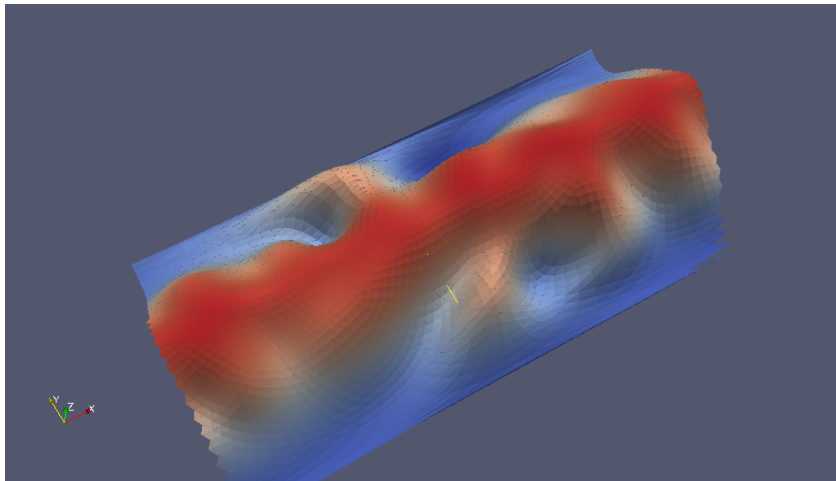
14



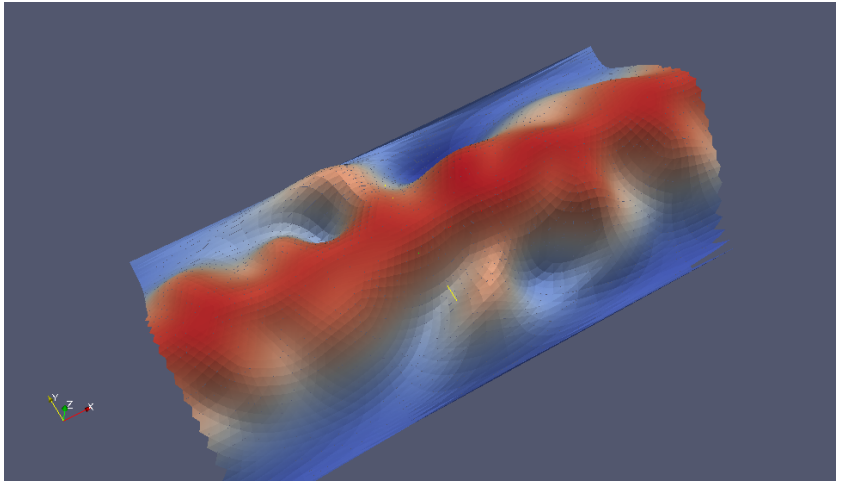
15



16

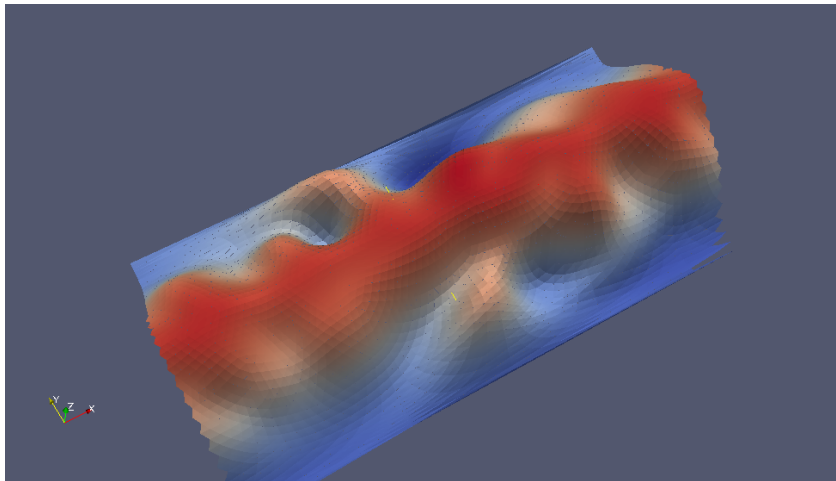


17

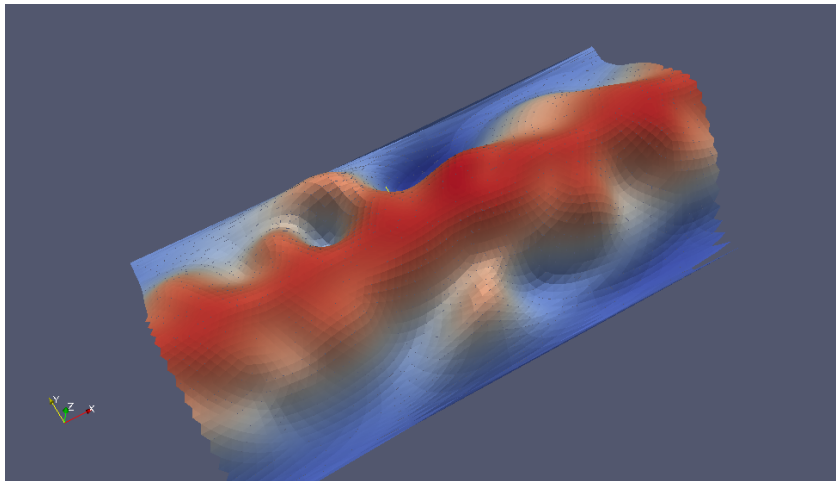


18

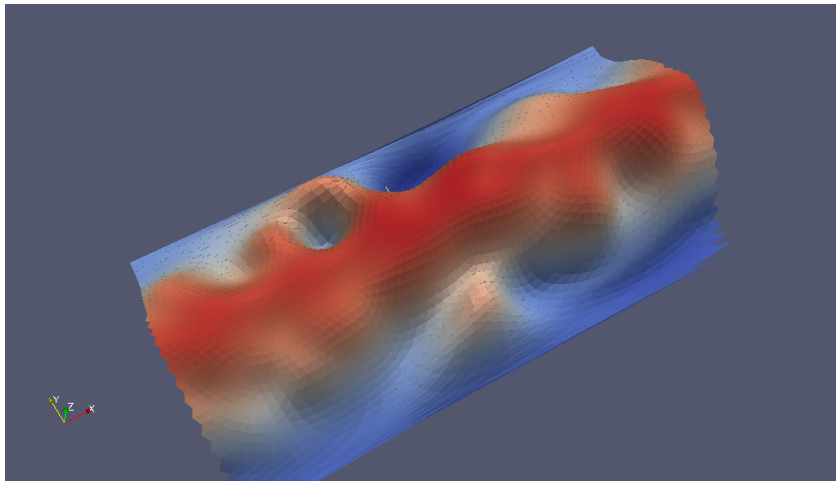




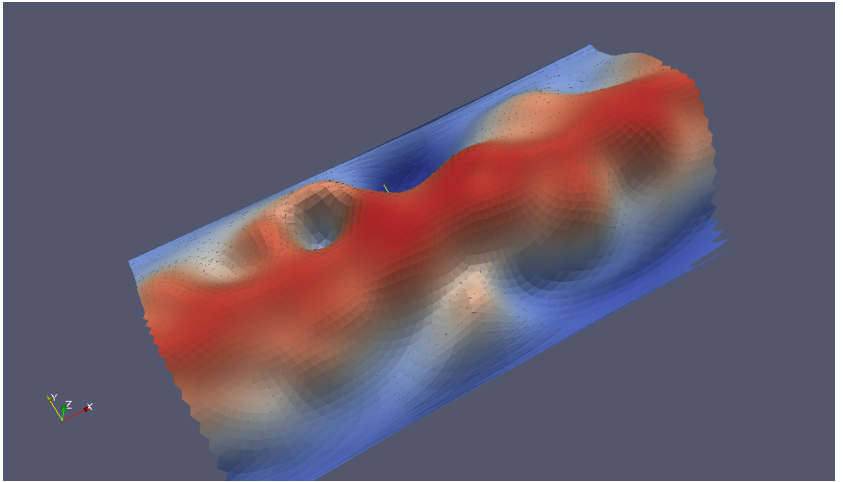
19



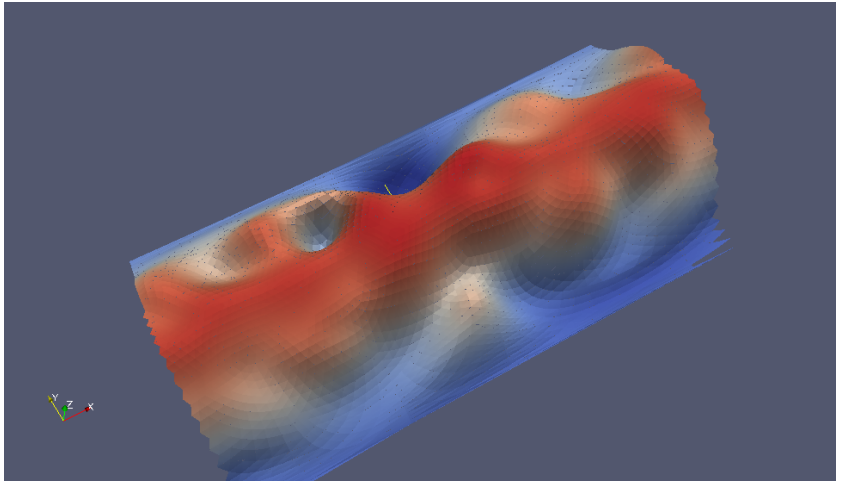
20



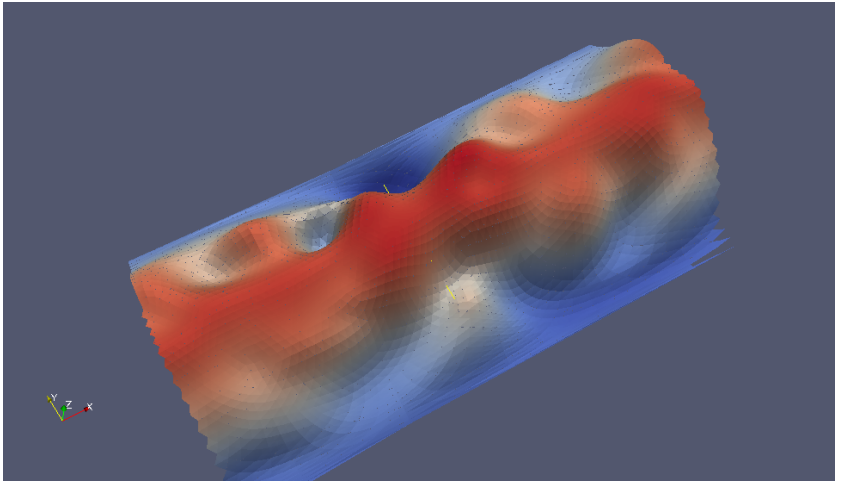
21



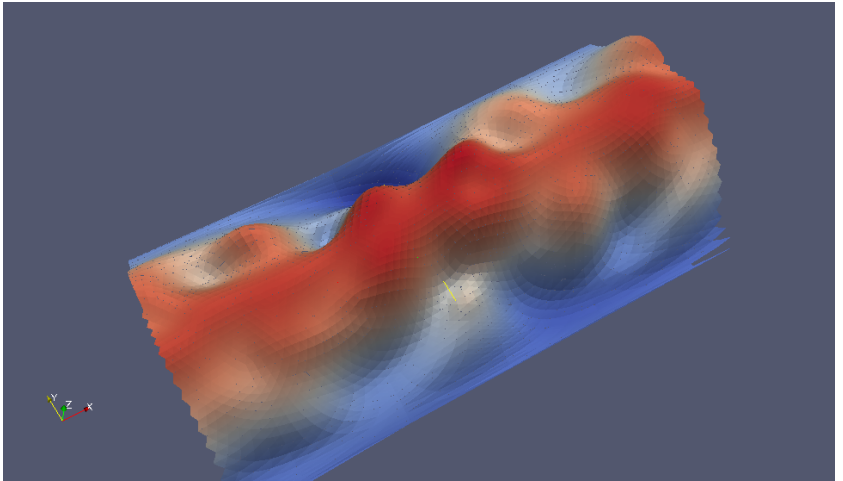
22



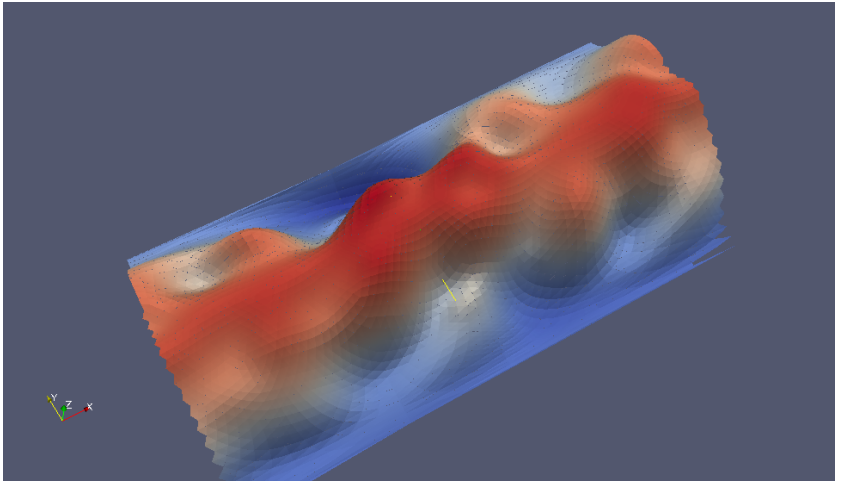
23



24

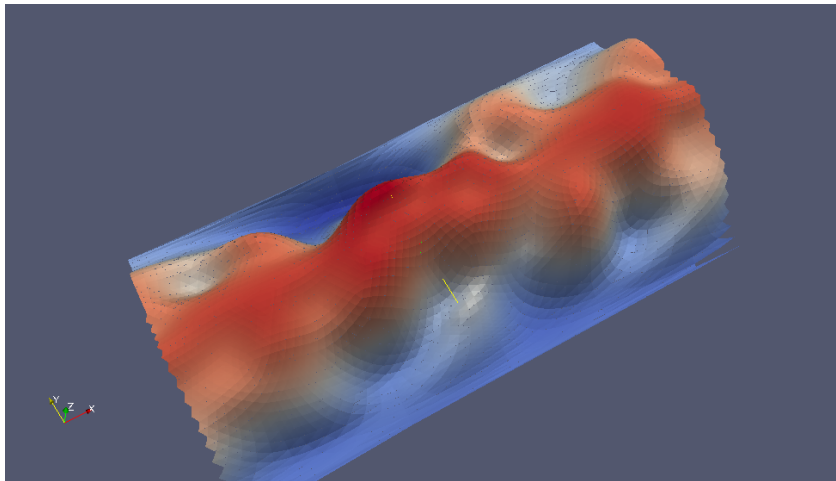


25

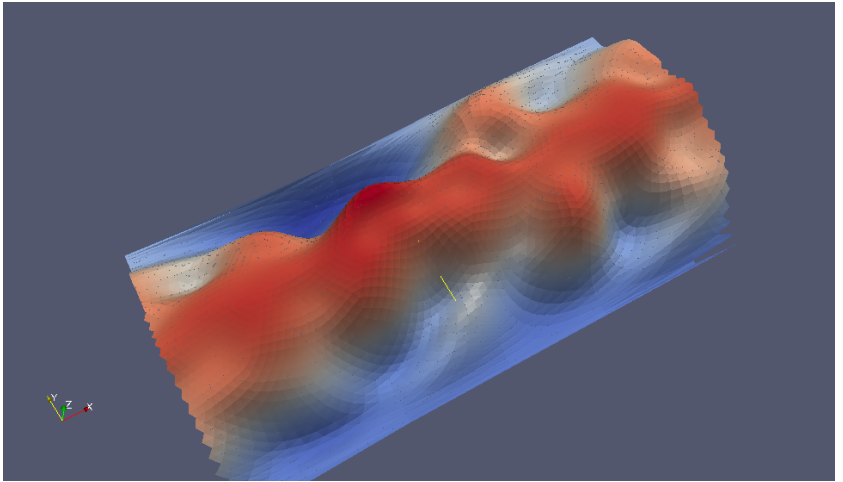


26

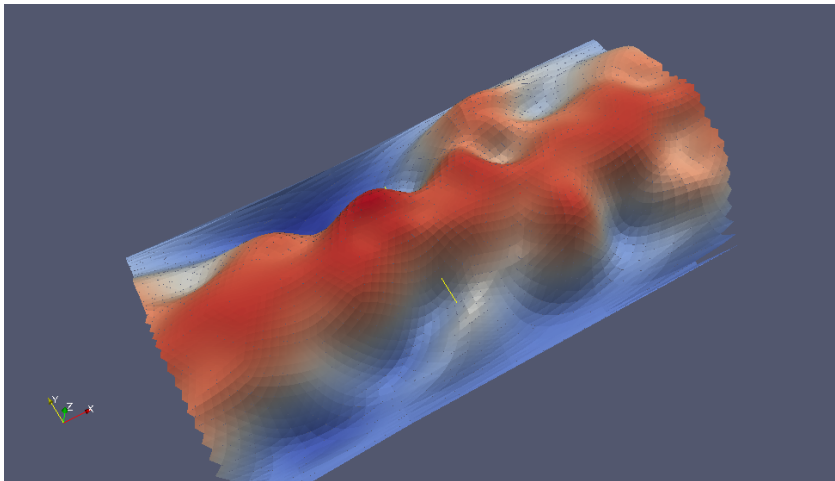




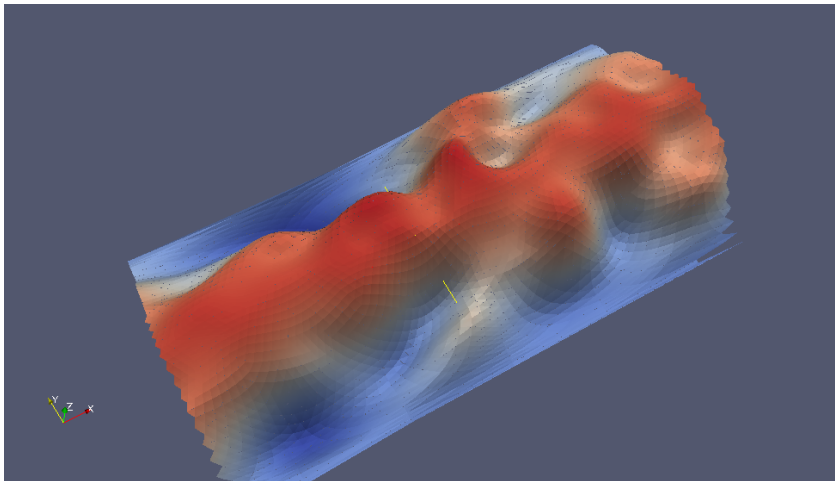
27



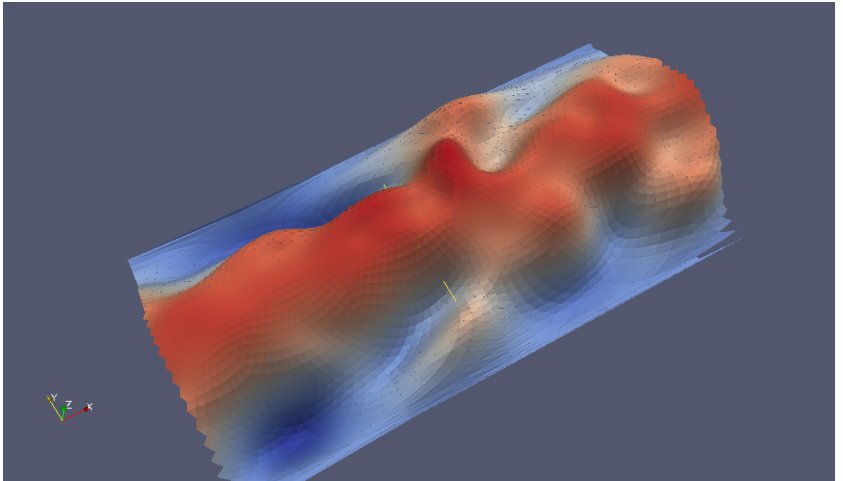
28



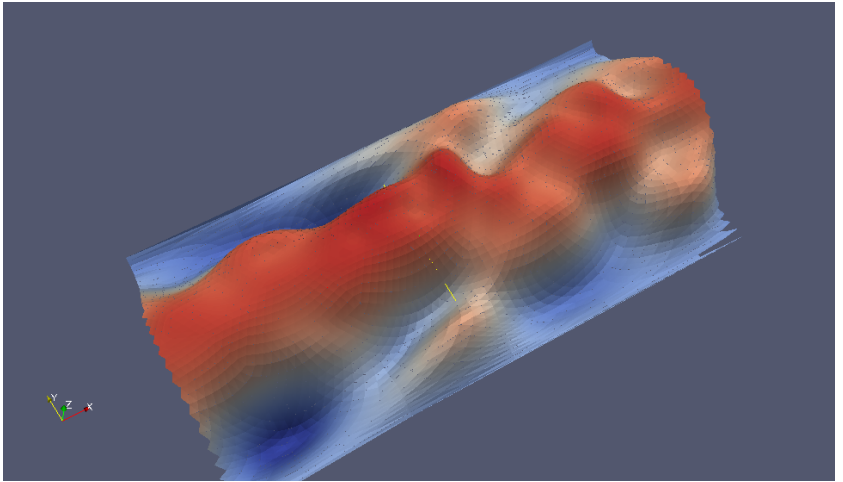
29



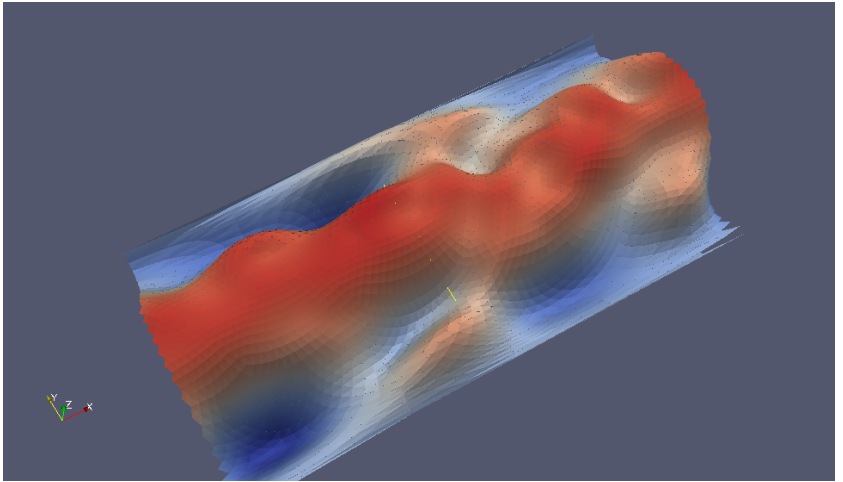
30



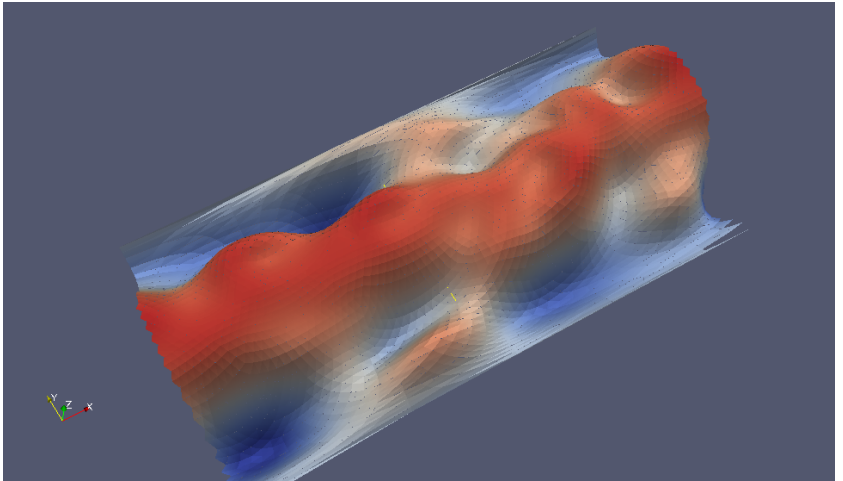
31



32

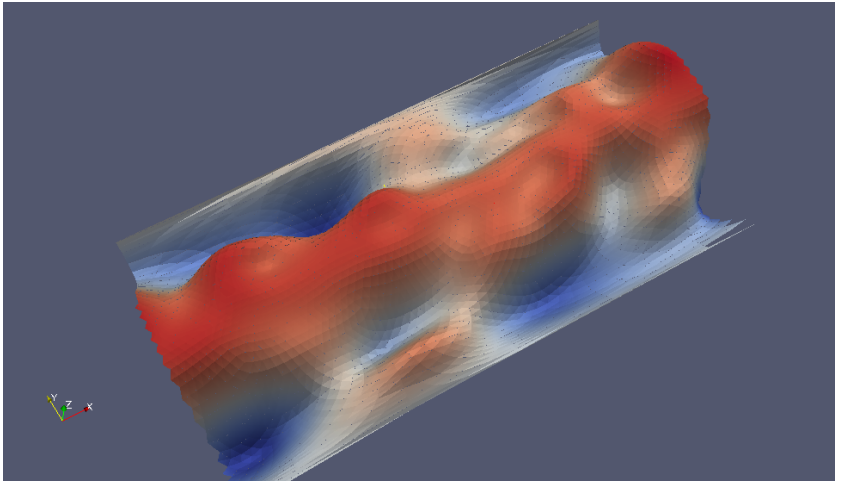


33

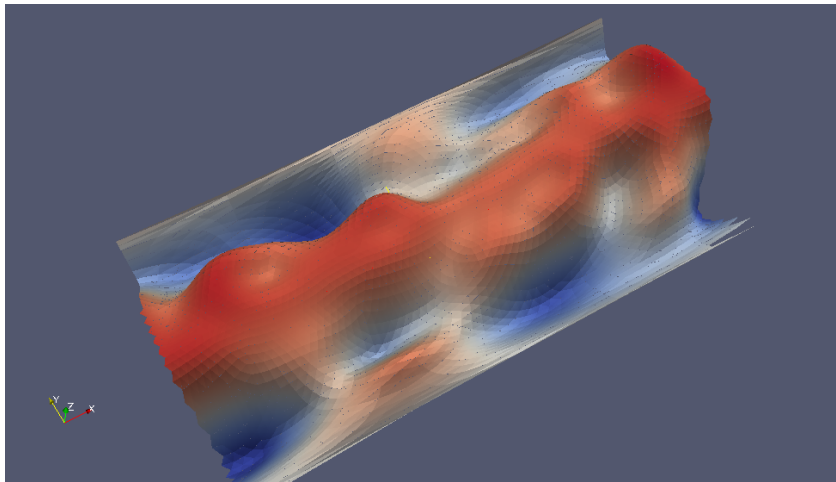


34

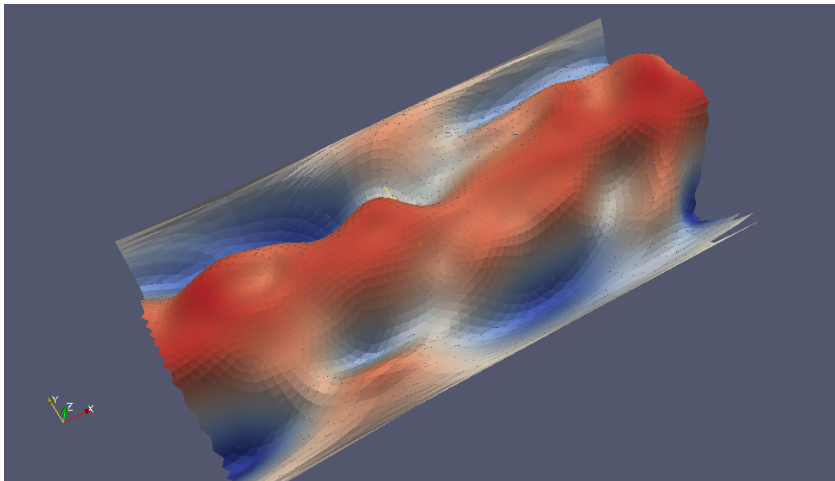




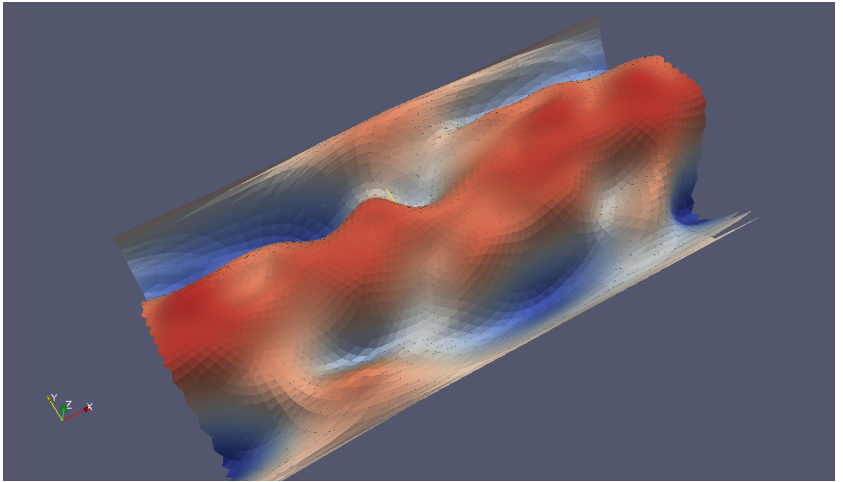
35



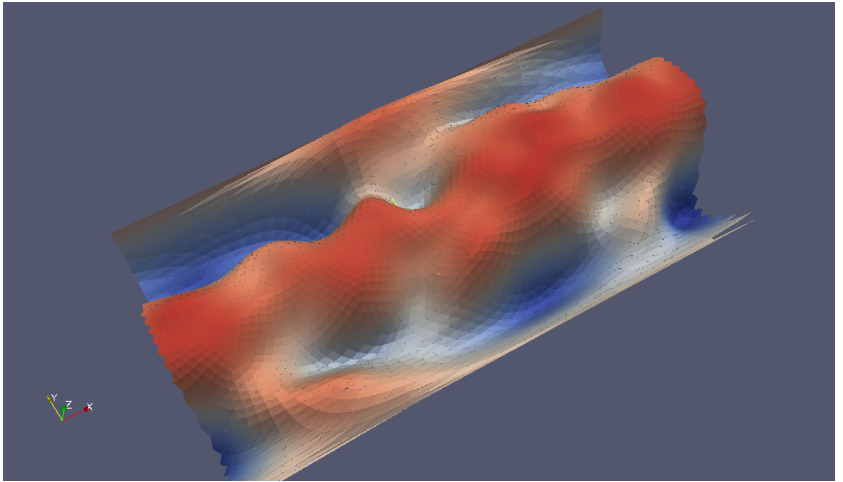
36



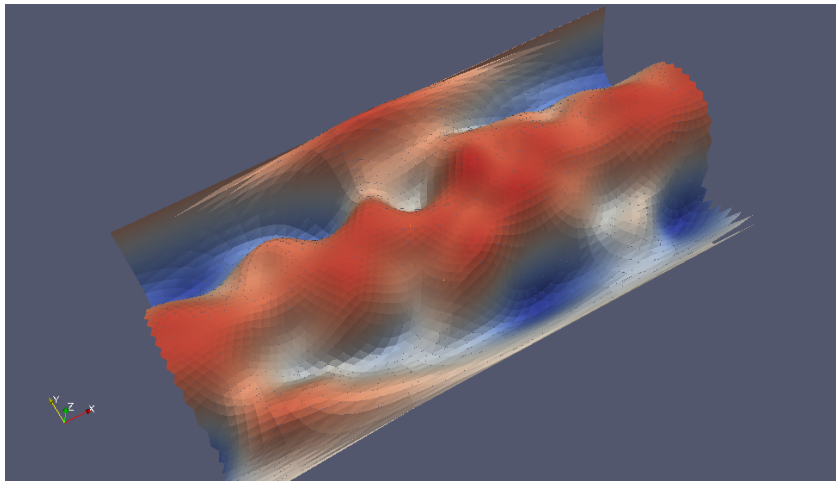
37



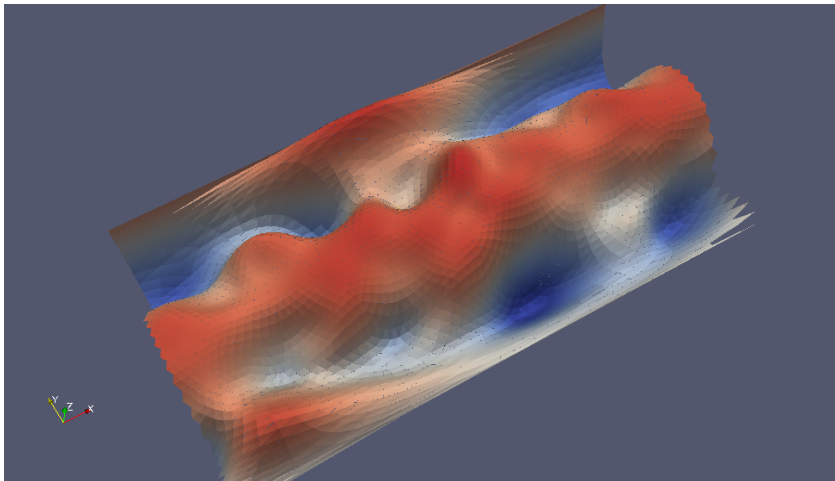
38



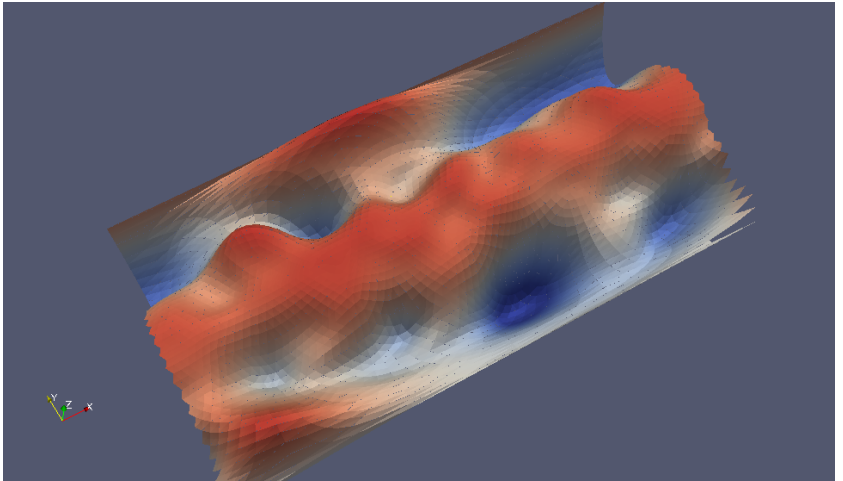
39



40

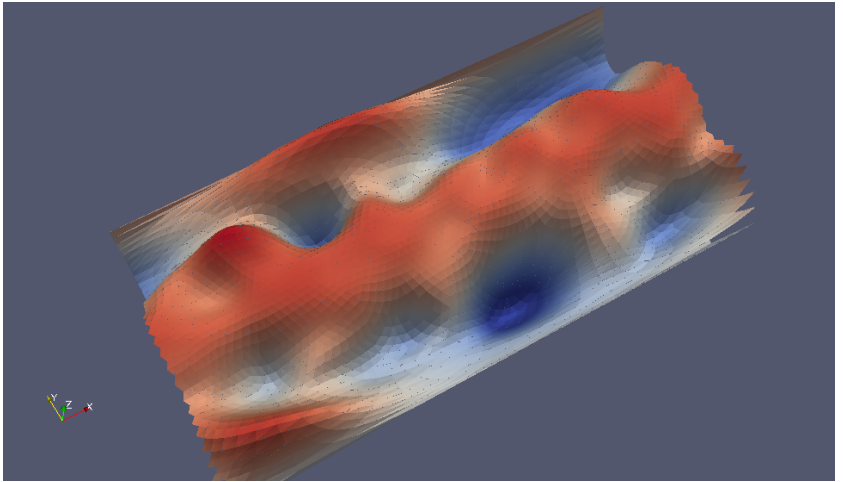


41

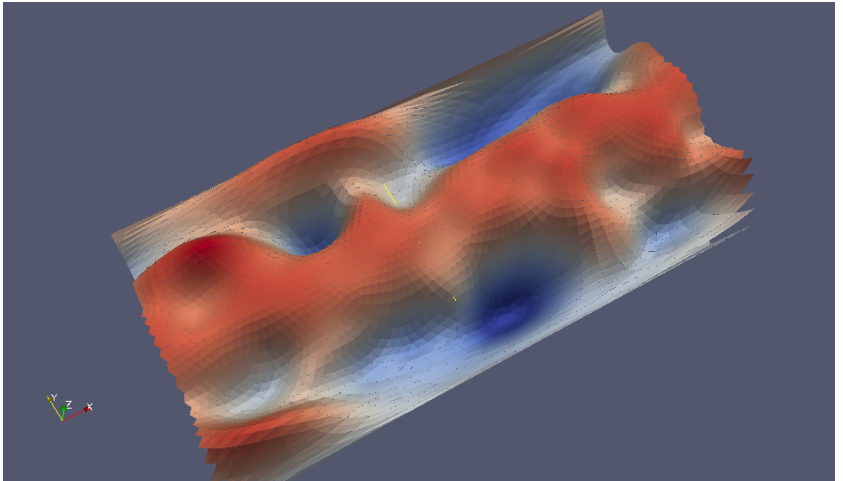


42

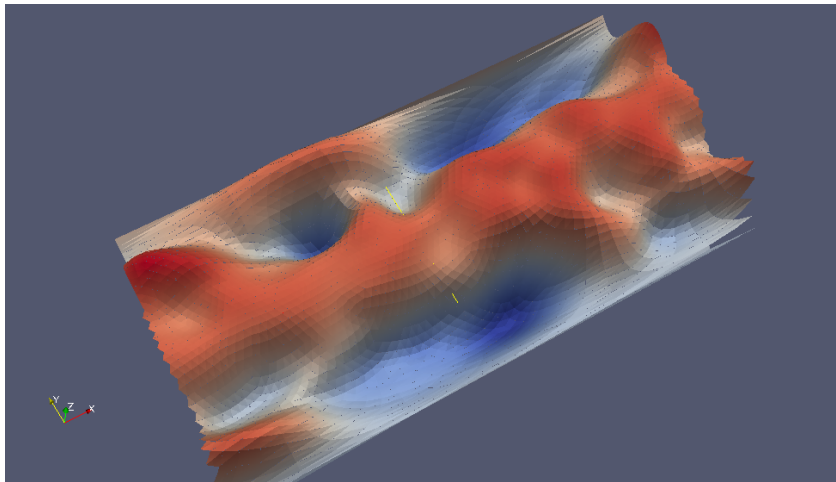




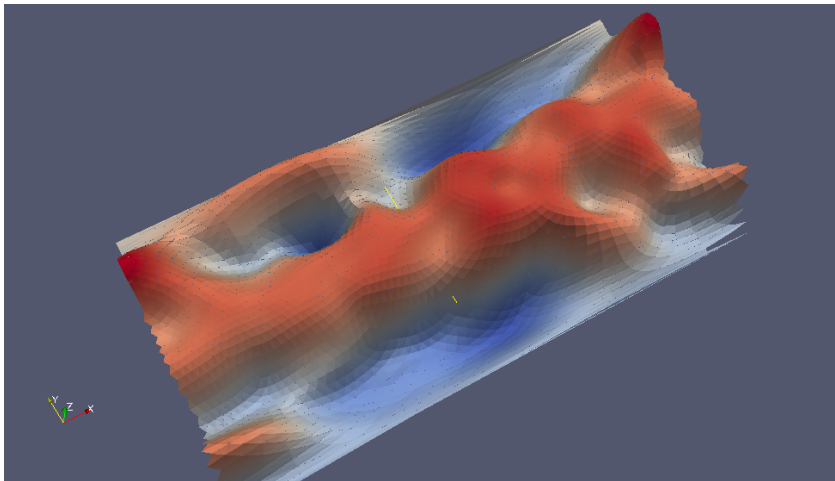
43



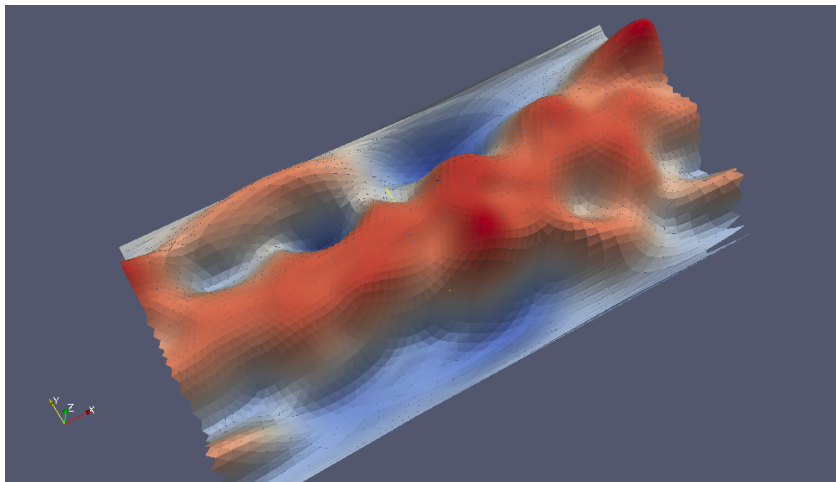
44



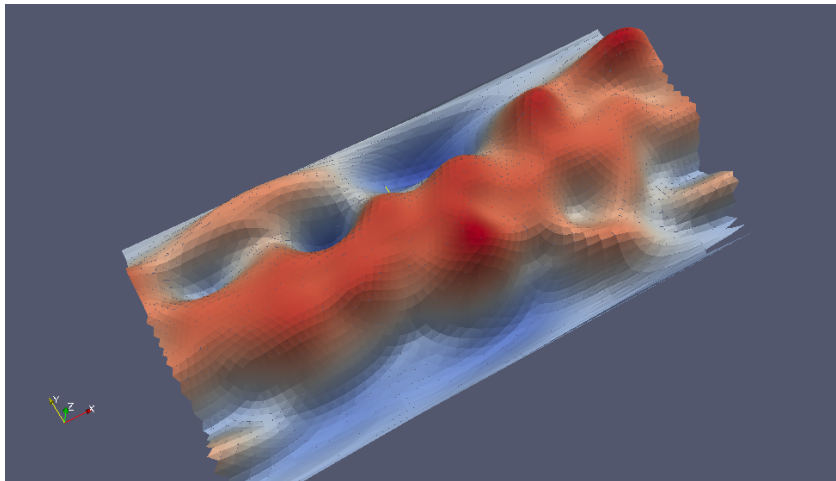
45



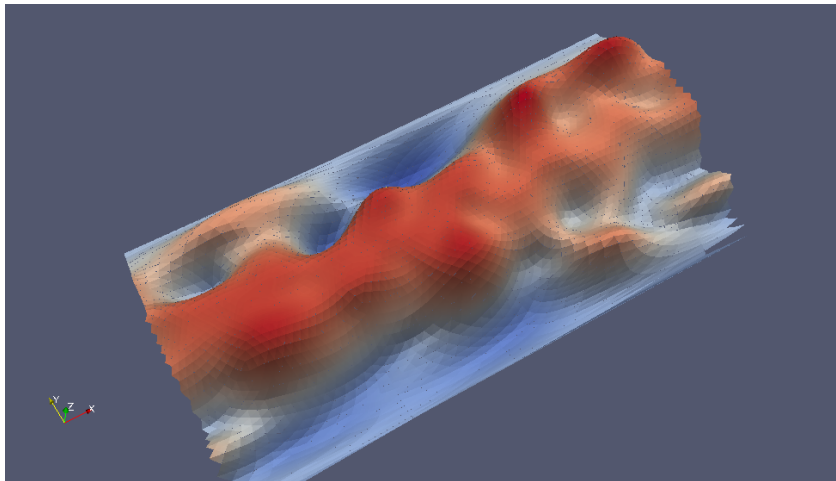
46



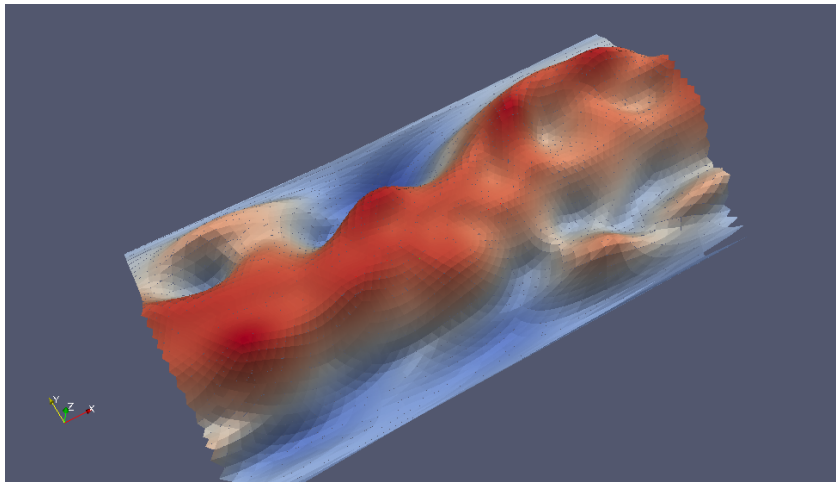
47



48

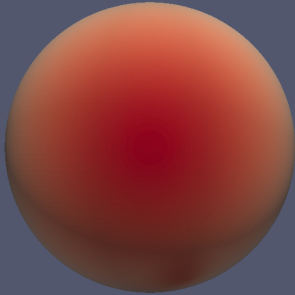


49

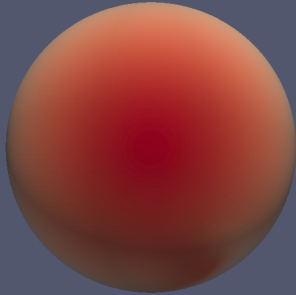


50

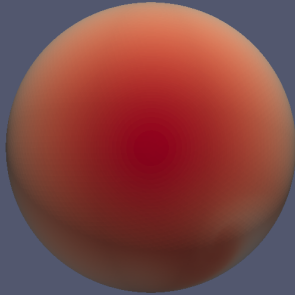




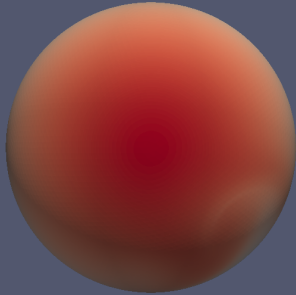
1



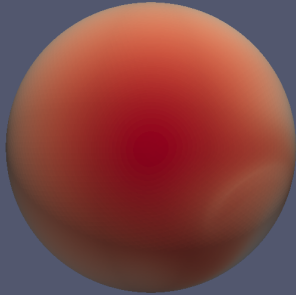
2



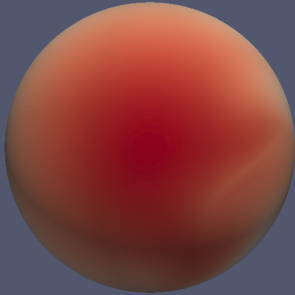
3



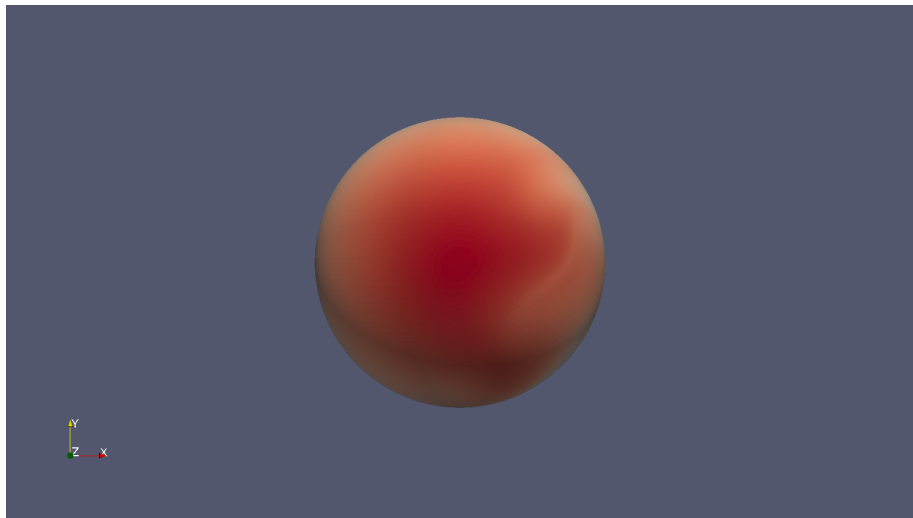
4



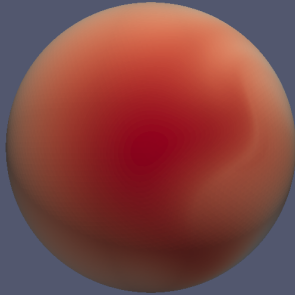
5



6

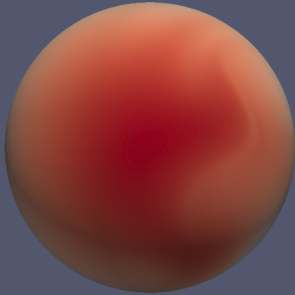


7

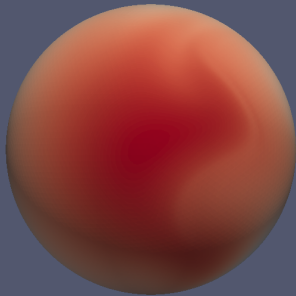


8

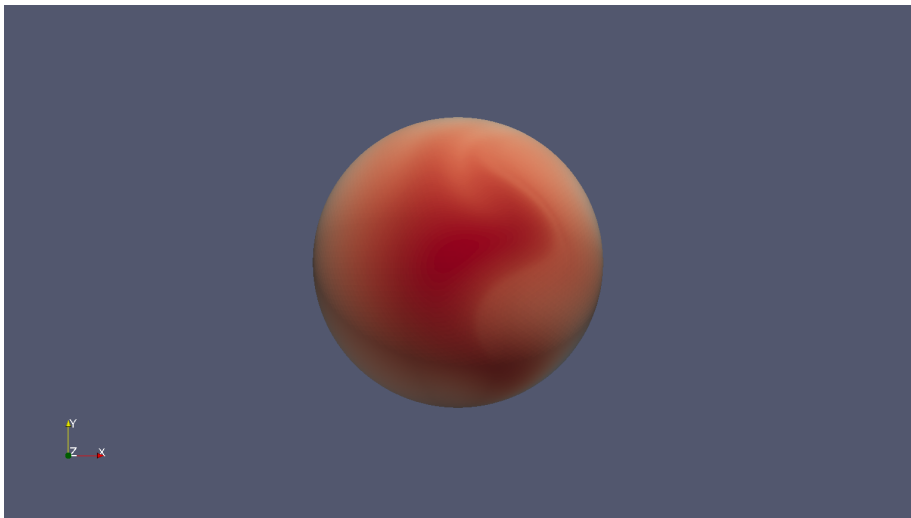




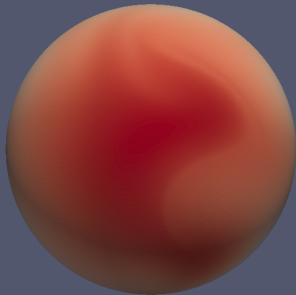
9



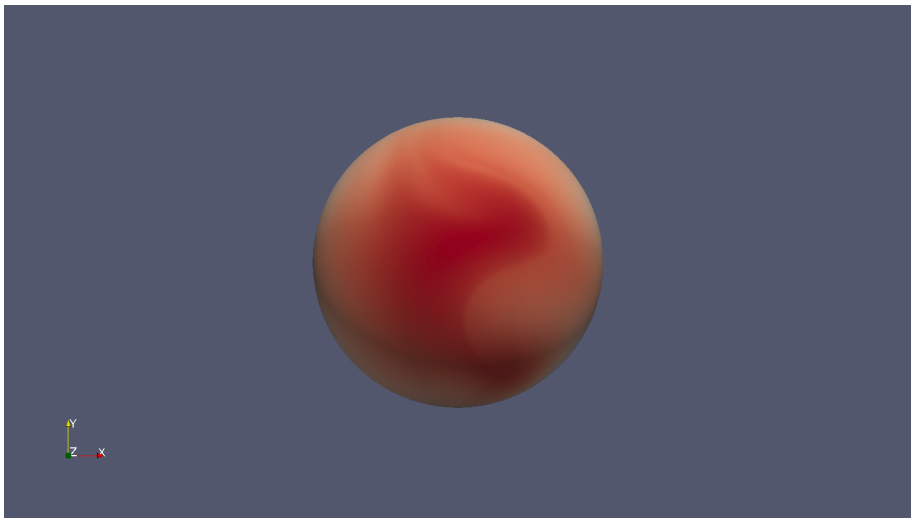
10



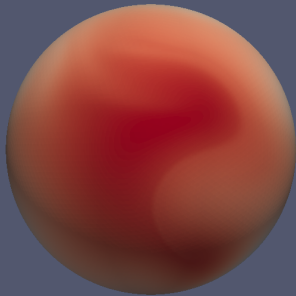
11



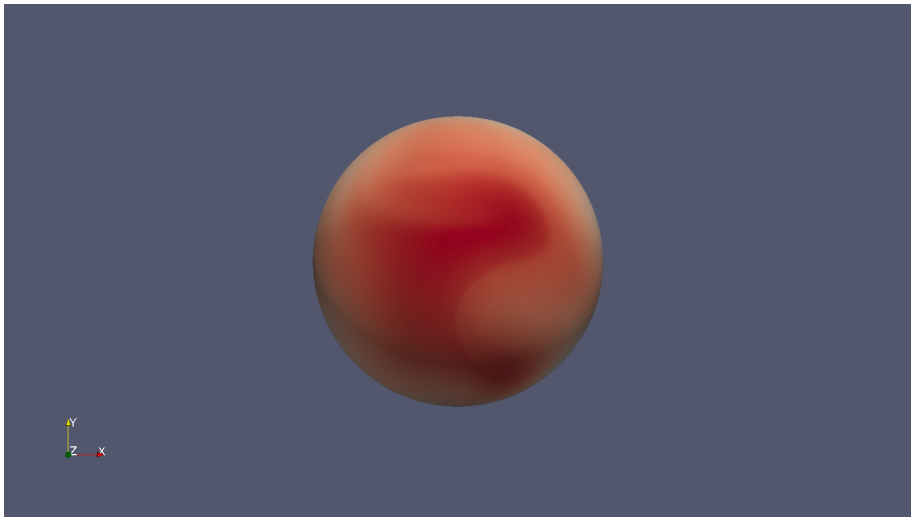
12



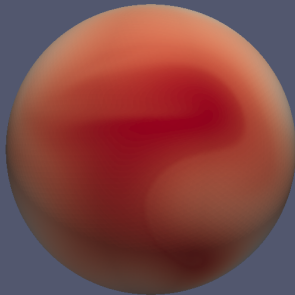
13



14

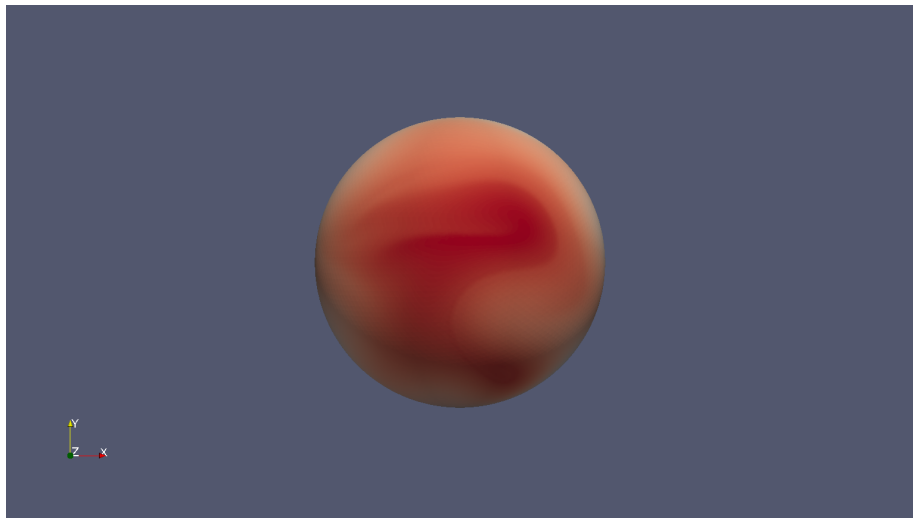


15

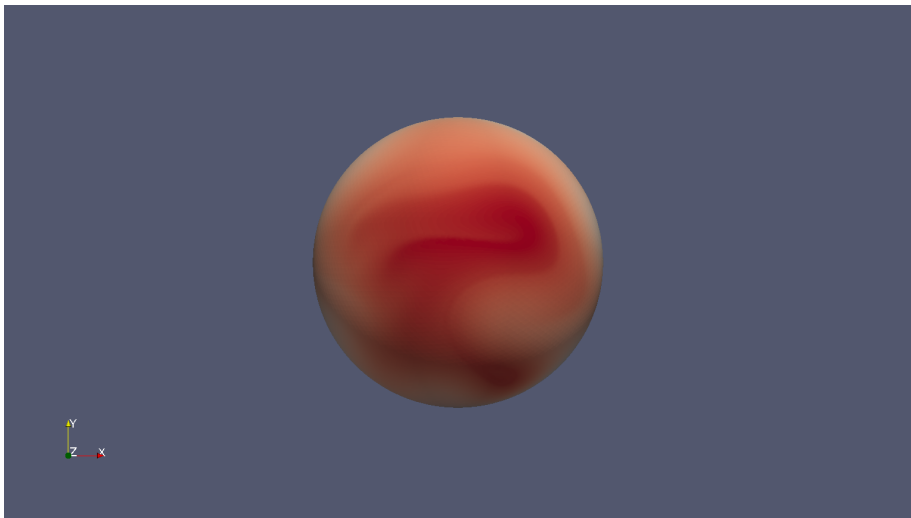


16

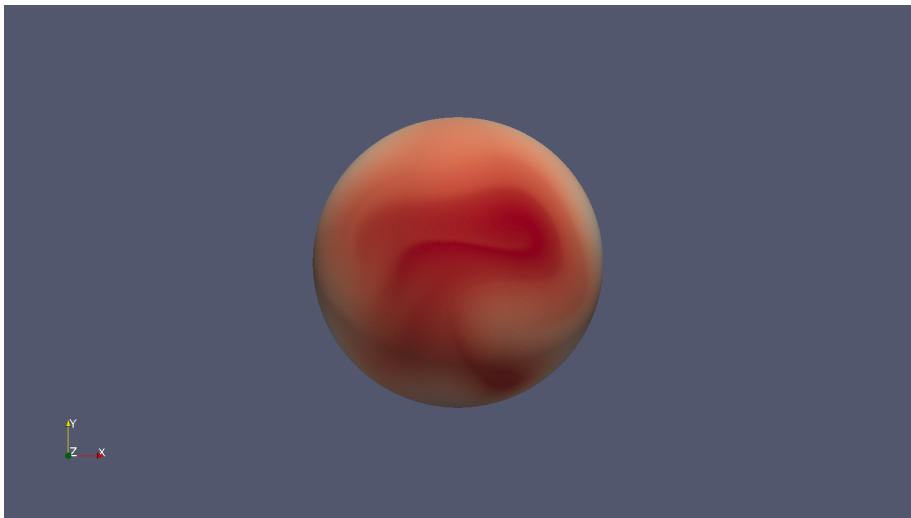




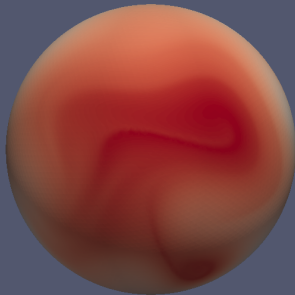
17



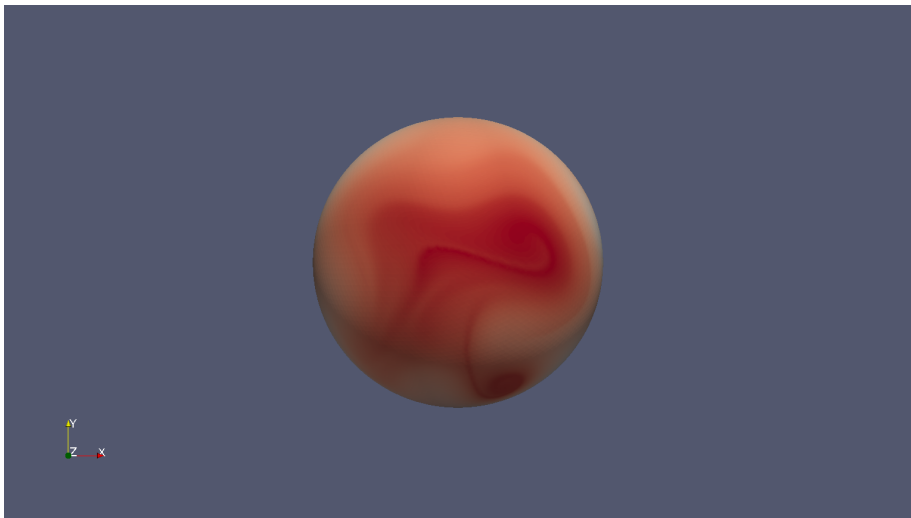
18



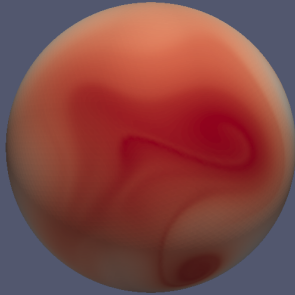
19



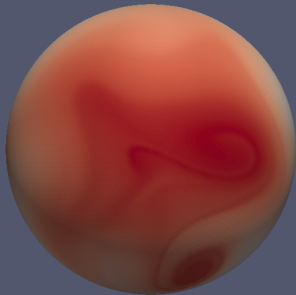
20



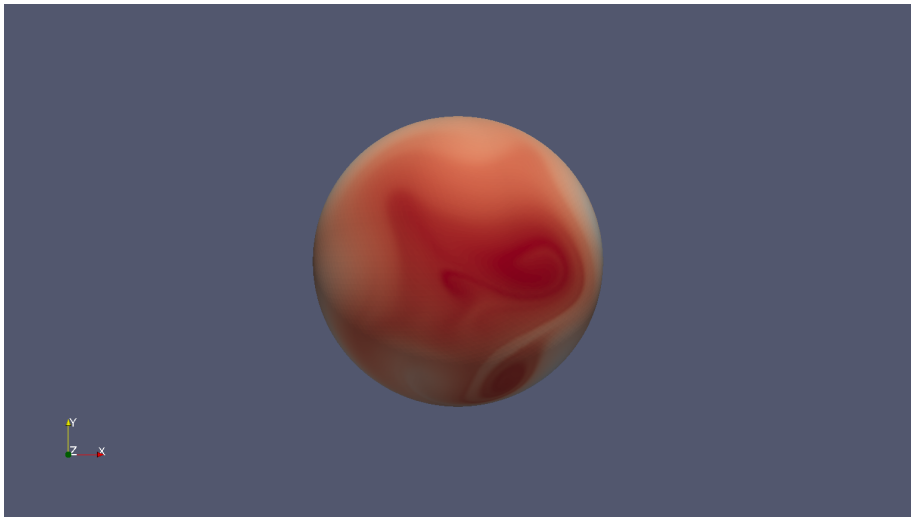
21



22

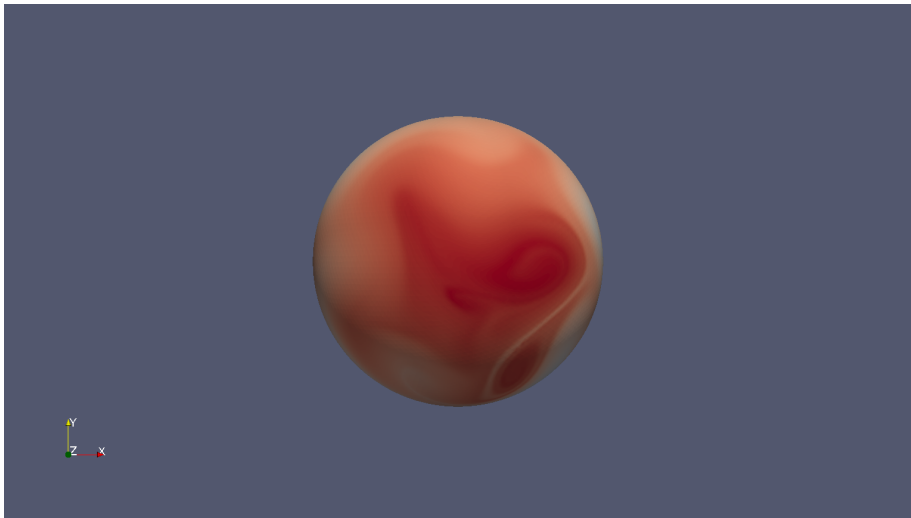


23

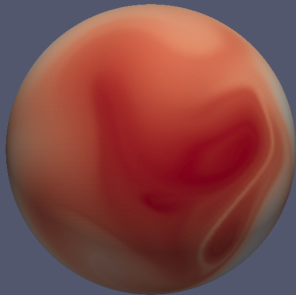


24

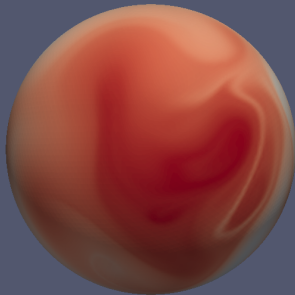




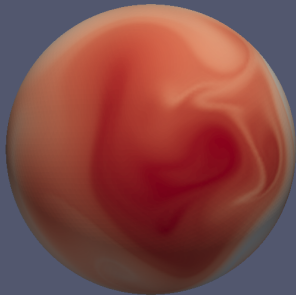
25



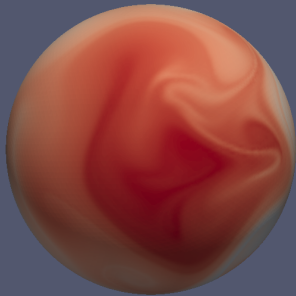
26



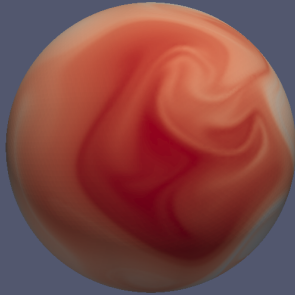
27



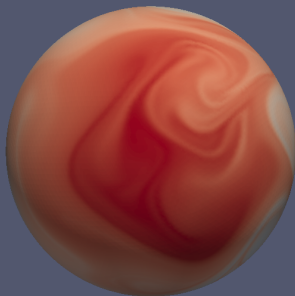
28



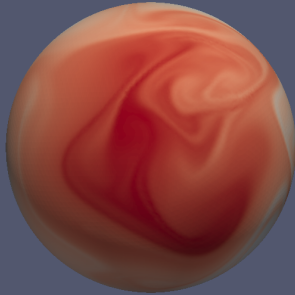
29



30

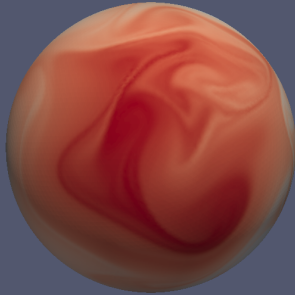


31

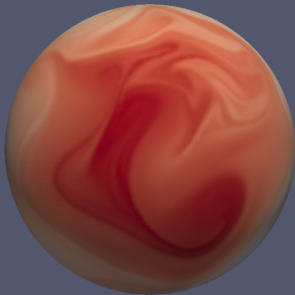


32

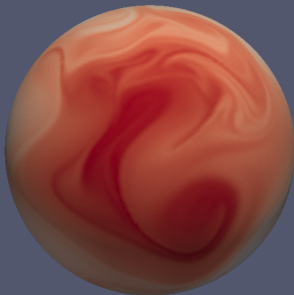




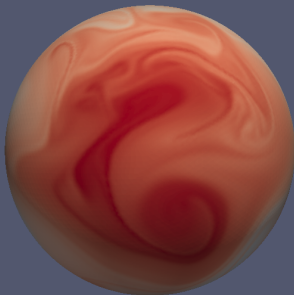
33



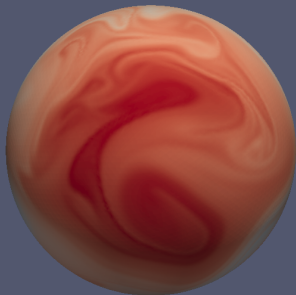
34



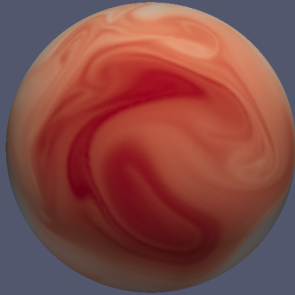
35



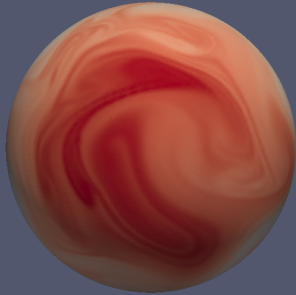
36



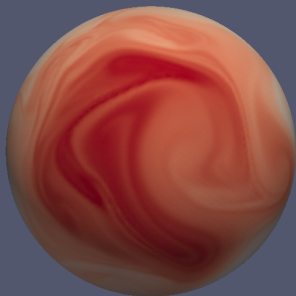
37



38

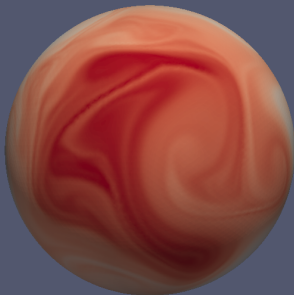


39

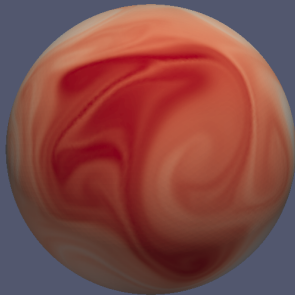


40

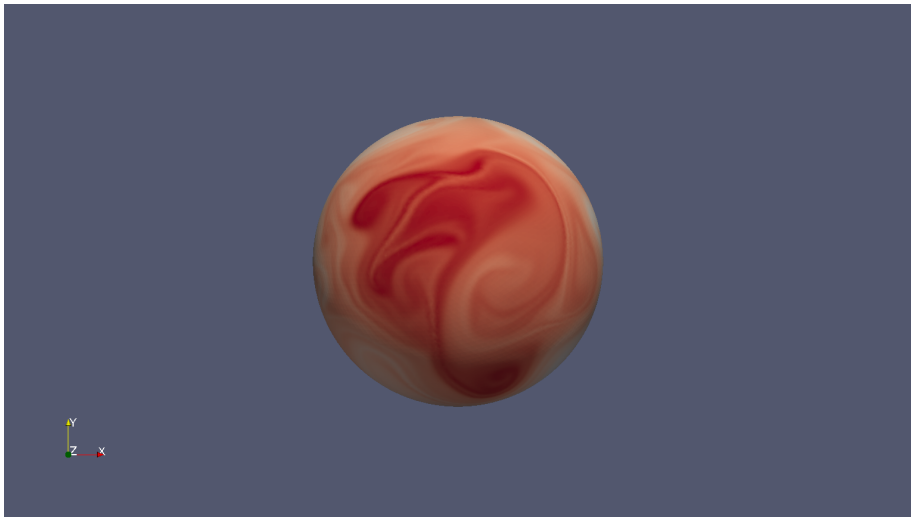




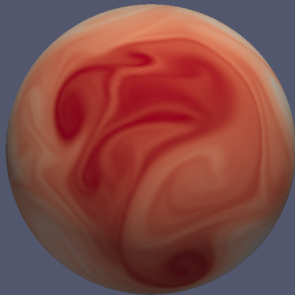
41



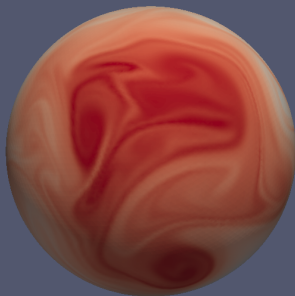
42



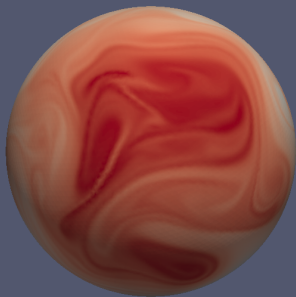
43



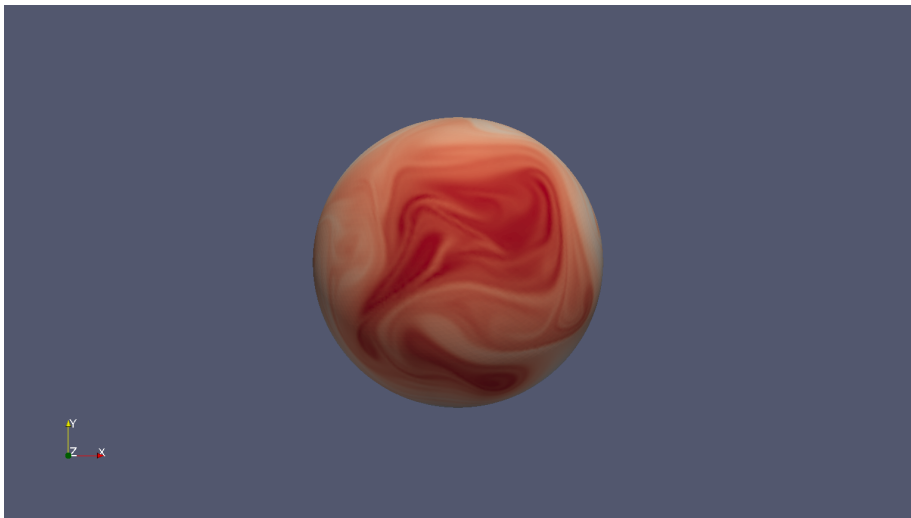
44



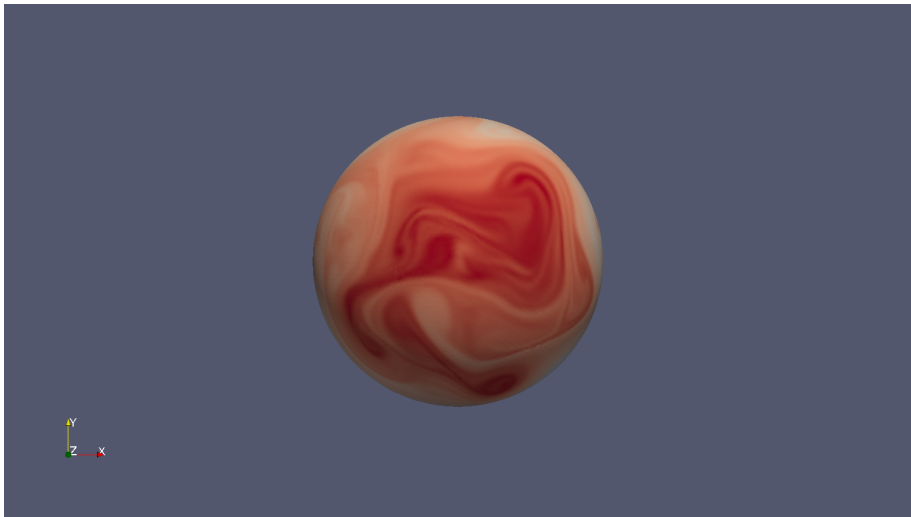
45



46

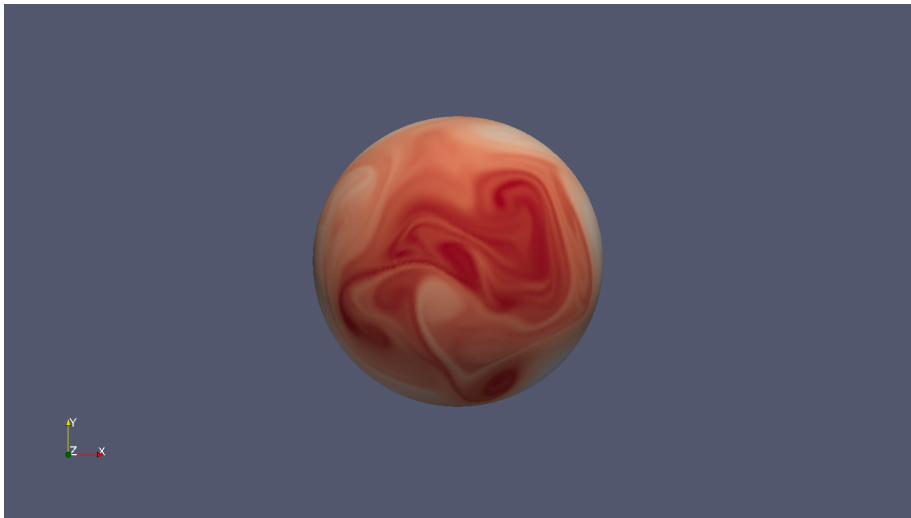


47

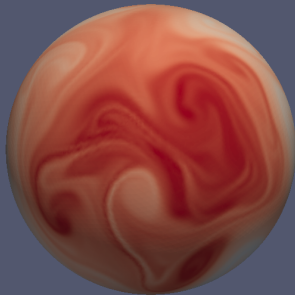


48





49



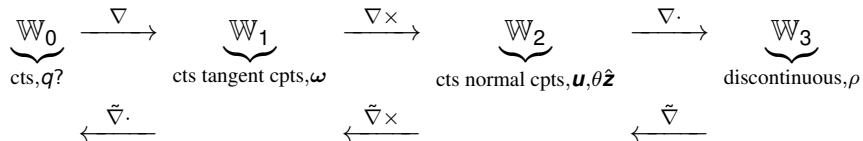
50

## Another story: dual meshes

$$\begin{array}{ccccc} & \xrightarrow{\tilde{\nabla}^\perp} & & \xrightarrow{\tilde{\nabla}^\cdot} & \\ \mathbb{V}_d^2 & \xleftarrow{\nabla^\perp \cdot} & \mathbb{V}_d^1 & \xleftarrow{\nabla \cdot} & \mathbb{V}_d^0 \\ \downarrow \star_h & & \downarrow \star_h & & \downarrow \star_h \\ \mathbb{V}_p^0 & \xrightarrow{\nabla^\perp} & \mathbb{V}_p^1 & \xrightarrow{\nabla \cdot} & \mathbb{V}_p^2 \\ & \xleftarrow{\tilde{\nabla}^\perp \cdot} & & \xleftarrow{\tilde{\nabla}^\cdot} & \end{array}$$

- J. Thuburn and CJC, *A framework for mimetic discretization of the rotating shallow-water equations on arbitrary polygonal grids*, SISC (2012).
- CJC and J. Thuburn, *A finite element exterior calculus framework for the rotating shallow-water equations*, (submitted to JCP, preprint on arXiv).

# Towards 3D



# Conclusions

- Extends C-grid approach with flexibility to take a) higher-order, b) non-orthogonal grids, c) different DOF ratios.
- Mimetic finite elements/finite element exterior calculus based on sequence of FE spaces compatible with  $\nabla^\perp$  and  $\nabla \cdot$  to retain  $\nabla \cdot \nabla^\perp = 0$ .
- Dual operators  $\tilde{\nabla}^\perp \cdot$  and  $\tilde{\nabla}$  are defined weakly and satisfy  $\tilde{\nabla}^\perp \cdot \tilde{\nabla}$ .
- Steady geostrophic modes and diagnostic PV conservation.
- Energy/entropy conservation possible.
- Efficient semi-implicit implementation with accurate advection is possible.

# References

- J. Thuburn and CJC, *A framework for mimetic discretization of the rotating shallow-water equations on arbitrary polygonal grids*, SISC (2012).
- CJC and J. Shipton, *Mixed finite elements for numerical weather prediction*, JCP (2012).
- A. Staniforth, T. Melvin and CJC, *Analysis of a mixed finite-element pair proposed for an atmospheric dynamical core*, QJRMS (2012).
- T. Melvin, A. Staniforth and CJC, *A two dimensional mixed finite element pair on rectangles*, to appear in QJRMS.
- CJC and J. Thuburn, *A finite element exterior calculus framework for the rotating shallow-water equations*, (submitted to JCP, preprint on arXiv).
- M. Rognes, CJC, D. Ham and A. McRae, *Automating the solution of PDEs on the sphere and other manifolds* (submitted to GMD, viewable on GMDD).
- A. McRae and CJC, *Energy-entropy conserving mixed finite element schemes for the rotating shallow water equations* (submitted to QJRMS, preprint on arXiv).

3 year postdoctoral research associate position available!